

Organic & Biomolecular Chemistry

Accepted Manuscript



This article can be cited before page numbers have been issued, to do this please use: D. Das, H. P.A. Khan, R. Shivahare, S. Gupta, J. Sarkar, I. Siddiqi, R. S. AMPAPATHI and T. K. Chakraborty, *Org. Biomol. Chem.*, 2017, DOI: 10.1039/C6OB02610A.



This is an Accepted Manuscript, which has been through the Royal Society of Chemistry peer review process and has been accepted for publication.

Accepted Manuscripts are published online shortly after acceptance, before technical editing, formatting and proof reading. Using this free service, authors can make their results available to the community, in citable form, before we publish the edited article. We will replace this Accepted Manuscript with the edited and formatted Advance Article as soon as it is available.

You can find more information about Accepted Manuscripts in the [author guidelines](#).

Please note that technical editing may introduce minor changes to the text and/or graphics, which may alter content. The journal's standard [Terms & Conditions](#) and the ethical guidelines, outlined in our [author and reviewer resource centre](#), still apply. In no event shall the Royal Society of Chemistry be held responsible for any errors or omissions in this Accepted Manuscript or any consequences arising from the use of any information it contains.

Journal Name

ARTICLE

Synthesis, SAR and biological studies of sugar amino acid based almiramide analogues: *N*-methylation leads the way

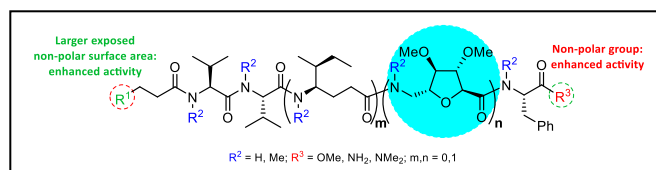
Received 00th January 20xx,
Accepted 00th January 20xx

DOI: 10.1039/x0xx00000x

www.rsc.org/

Dipendu Das,^a Hina P. A. Khan,^b Rahul Shivahare,^c Suman Gupta,^c Jayanta Sarkar,^d Mohd. Imran Siddiqui,^e Ravi Sankar Ampapathi,^{*f} Tushar Kanti Chakraborty^{*b}

Leishmaniasis, caused by the protozoan parasites of the genus *Leishmania*, is one of the most neglected diseases endemic in many continents posing enormous global health threats and therefore, the discovery of new antileishmanial compounds is of utmost urgency. Antileishmanial activities of a library of sugar amino acid based linear lipopeptide analogues have been examined with the aim to identify potential drug candidates to treat visceral leishmaniasis and we were pleased to find that among the synthesized analogues most of the permethylated compounds exhibited more activity in *in vitro* studies against intra-macrophagic amastigotes than its non-methylated analogues. SAR and NMR studies revealed that introduction of the *N*-methyl groups inhibited the formation of any turn structure in these molecules that led to improved activities.



Introduction

Leishmaniasis, one of the “most neglected diseases”¹ caused by protozoan parasites belonging to the genus *Leishmania*, is transmitted to human through the bite of female phlebotomine sand flies infected with the parasites.² It is a geographically widespread disease prevalent in many parts of the tropical and subtropical world causing significant morbidity or mortality.³ This disease is a severe public health problem in many developing countries of East Africa, the Indian subcontinent and Latin America.

Antileishmanial therapy relies on handful of drugs such as, the first-line treatment option involving the administration of meglumine antimonate (MA), sodium stibogluconate (SSG) and amphotericin B.⁴ Second-line drugs include miltefosine, and

paromomycine.⁵ However, the treatment with these existing drugs suffers from several limitations such as cost, high toxicity, difficulty in administration and spread of drug resistance.⁶ Therefore, there is still a crying need of new efficacious and safe drugs based on new molecular scaffold in the absence of any upcoming vaccine.⁷ Among the different heterocyclic structures that have been disclosed, the nitrogen containing compounds found in many natural products are the source of some important lead molecules.⁸

The *N*-methylated lipopeptides, almiramides A-C (**1-3**) (Figure 1) are marine natural products, originally isolated from a Panamanian collection of *Lyngbya majuscula* in conjunction with the Panama International Cooperative Biodiversity Group (ICBG).^{8c,9} This class of natural products was found to be active against *Leishmania donovani*, the causative agent of leishmaniasis and also showed activity against the related kinetoplastid parasite *Trypanosoma brucei*, the causative agent of human African trypanosomiasis. Target identification studies indicated that the almiramides likely perturb glycosomal function through disruption of membrane assembly machinery.⁹

The encouraging pharmacological profiles of almiramides as peptide based lead molecules having antileishmanial activity prompted us to target almiramides for further drug development and also to explore the SARs by preparing their analogues.

^a Medicinal & Process Chemistry Division, CSIR-Central Drug Research Institute, Sector 10, Jankipuram Extension, Sitapur Road, Lucknow 226031, India.

^b Department of Organic Chemistry, Indian Institute of Science, CV Raman Road, Bengaluru 560012, India.

^c Parasitology Division, CSIR-Central Drug Research Institute, Sector 10, Jankipuram Extension, Sitapur Road, Lucknow 226031, India.

^d Biochemistry Division, CSIR-Central Drug Research Institute, Sector 10, Jankipuram Extension, Sitapur Road, Lucknow 226031, India.

^e Molecular and Structural Biology Division, CSIR-Central Drug Research Institute, Sector 10, Jankipuram Extension, Sitapur Road, Lucknow 226031, India.

^f Centre for Nuclear Magnetic Resonance, SAIF, CSIR-Central Drug Research Institute, Sector 10, Jankipuram Extension, Sitapur Road, Lucknow 226031, India
Electronic Supplementary Information (ESI) available: NMR spectra and molecular dynamics. See DOI: 10.1039/x0xx00000x

In recent years, the interest in rational design of peptidomimetics has steadily grown due to the pharmacological limitations of bioactive natural peptides. A large variety of peptide modifications have been used for conformationally directed drug design to investigate the active peptide-receptor binding interactions. For this purpose, wide ranging structurally rigid non-peptidic molecular scaffolds have been designed. Insertion of these moieties in appropriate sites to restrict the conformational degrees of freedom in peptides produces the specific 3D structures required for binding their receptors. Sugar amino acids (SAA) belong to one such class of conformationally constrained templates that have been used extensively in many peptidomimetic studies.¹⁰ Linington and co-workers have synthesized a library of synthetic analogues of almiramides **1-3** and checked their biological activity in parallel with the original lead compounds, and identified several new

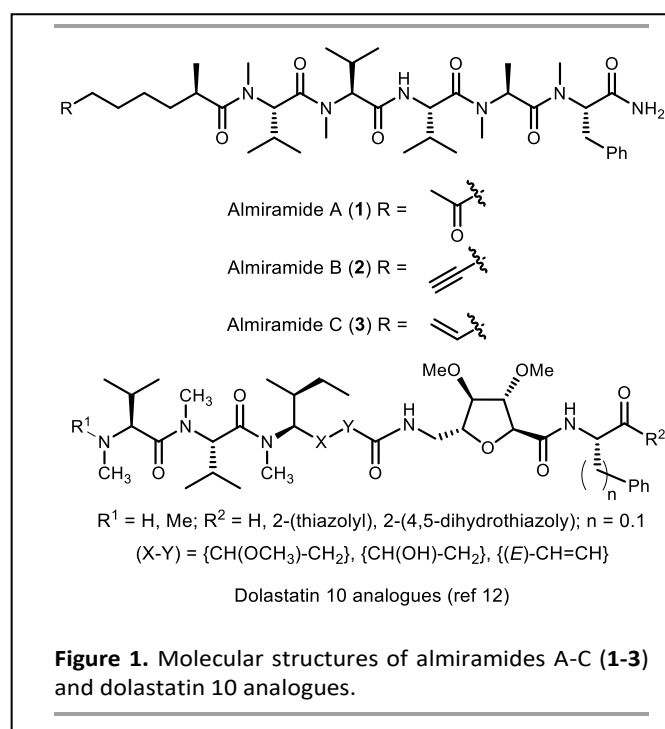


Figure 1. Molecular structures of almiramides A-C (**1-3**) and dolastatin 10 analogues.

structures with comparable activities to the original natural products.^{8c,9}

Our interests in the use of SAAs as dipeptide isosteres in peptidomimetic studies¹¹ prompted us to synthesize a small library of almiramide analogues by incorporating furanoid sugar amino acid in the backbone replacing some of its constituent amino acids to prove the viability of this template in discovering antileishmanial leads for future medicinal chemistry and drug development.

Results and Discussion

Chemistry. A series of 23 compounds with a general structure **4** (**4A-W**, Figure 2) having hybrid sequences of natural amino acids (AAs), unnatural (4*R*,5*S*)-4-amino-5-methylheptanoic acid (AMH)

View Article Online
DOI: 10.1039/C6OB02610A

Compound	R ¹	R ²	R ³	m,n
4A		H	OMe	1,1
4B		H	NH ₂	1,1
4C		Me	NMe ₂	1,1
4D		H	OMe	1,0
4E		H	NH ₂	1,0
4F		H	OMe	0,1
4G		H	NH ₂	0,1
4H		Me	NMe ₂	0,1
4I		H	OMe	0,1
4J		H	NH ₂	0,1
4K		Me	NMe ₂	0,1
4L		H	OMe	0,1
4M		H	NH ₂	0,1
4N		Me	NMe ₂	0,1
4O		H	OMe	0,1
4P		H	NH ₂	0,1
4Q		Me	NMe ₂	0,1
4R		H	OMe	0,1
4S		H	NH ₂	0,1
4T		Me	NMe ₂	0,1
4U	Ph	H	OMe	0,1
4V	Ph	H	NH ₂	0,1
4W	Ph	Me	NMe ₂	0,1

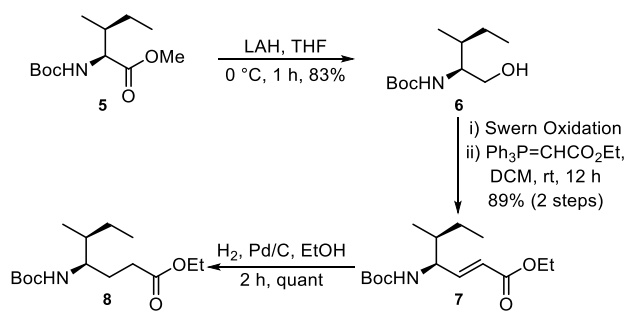
Figure 2. Structures of the designed analogues (**4A-W**).

and a mannose-derived sugar amino acid (MAA) were synthesized to screen against *L. donovani*. These compounds were derived from our earlier reported potent dolastatin 10 analogues (Figure 1) that

were shown to have excellent tubulin binding properties strongly suppressing the dynamics of microtubule assembly *in vitro*.¹² The fact that mammalian tubulin binding cytotoxic molecules have been widely screened against kinetoplastid tubulin for discovering anti-leishmanial compounds¹³ prompted us to screen our dolastatin 10 analogues for their antileishmanial activities as well. In addition, these dolastatin 10 analogues also showed synergistic effect with colchicine lending further support to screen them for antileishmanial activities as colchicine is known for its strong binding with β -tubulin of *Leishmania spp.*¹⁴ Subsequent discovery of almiramides A-C was of immense help for remodelling the dolastatin 10 analogues into almiramide look-alikes for the present study. The basic peptide skeleton of the parent dolastatin 10 analogues was retained in three compounds **4A-C** with insertions of only the *N*-acyl groups. The dipeptide isosteric MAA essentially

only one of these building blocks – **4A-C** having both MAA and AMH, **4D-E** having only AMH and **4F-W** having only MAA.

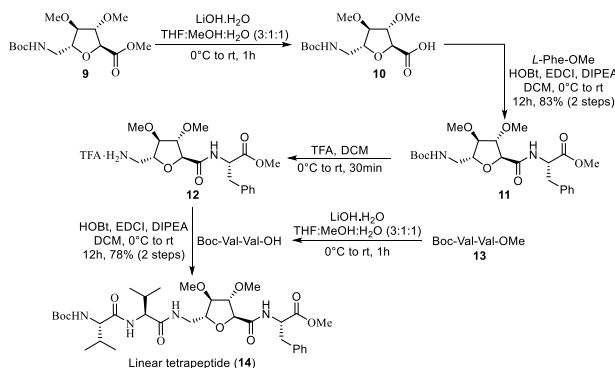
Scheme 1. Synthesis of the modified isoleucine unit 8



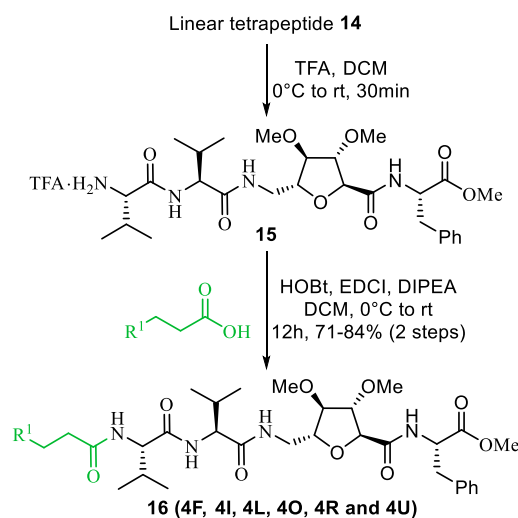
replaced the Val-Ala segment of almiramides. As Val is known to maximally stabilize secondary structures in peptides, replacement of only one Val was assumed not to cause any major conformational change. The presence of Phe in the C-terminus of dolastatin 10 analogues suitably conformed to the C-terminus of almiramides.

To assess the effects of the unnatural amino acids, the conformationally restrained δ -amino acid MAA and flexible γ -amino acid, (4*R*,5*S*)-4-amino-5-methylheptanoic acid (AMH) on the activities of these molecules, analogues were made with both or

Scheme 2. Synthesis of the linear tetrapeptide 14



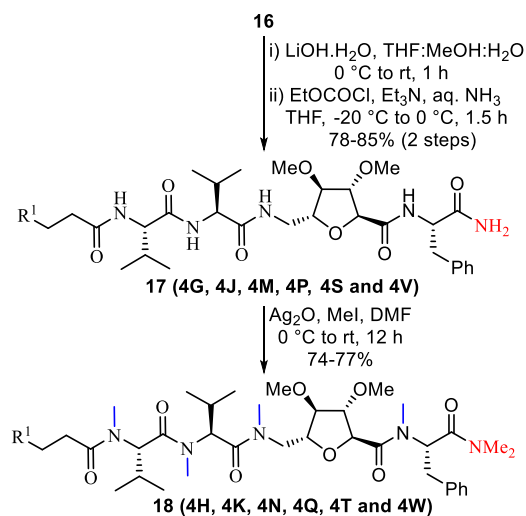
Scheme 3. Attachment of the lipophilic chains

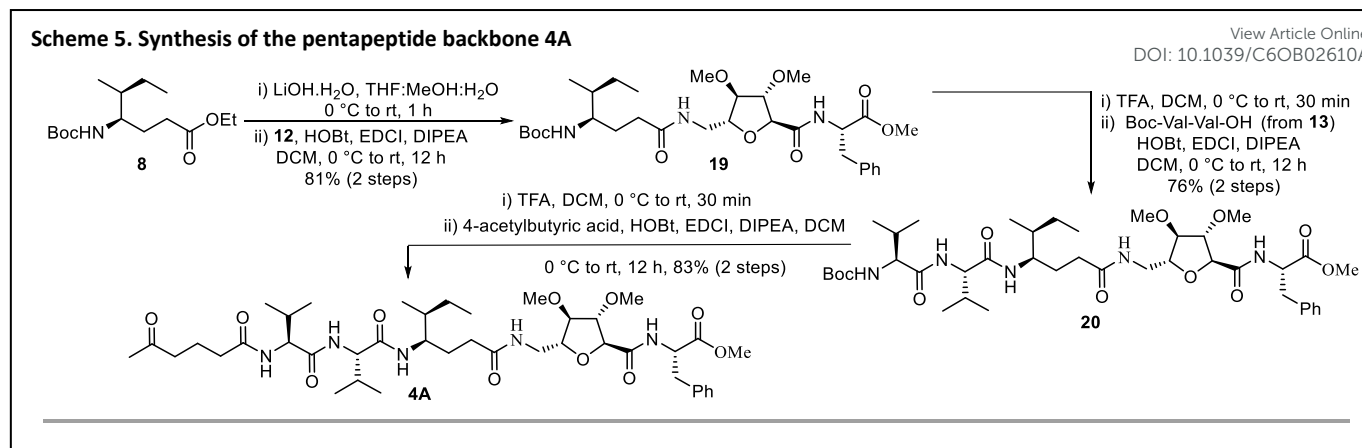


Synthesis of the monomeric building blocks. For the synthesis of the almiramide analogues, represented by a general formula **4** (Figure 2), the differentially protected peptidomimetic building blocks **8**, **9** (Schemes 1 and 2) and other natural amino acids were employed.

The synthesis of the protected monomeric unit Boc-AMH-OMe (**8**) started from the Boc-L-isoleucine methyl ester (**5**, Scheme 1).¹³ First, reduction of the ester group by LAH provided the alcohol **6** which was oxidized using Swern condition¹⁵ followed by 2-carbon olefination to furnish the α,β -unsaturated ester **7**.¹⁶ Hydrogenation of **7** delivered the required monomeric unit **8**. Synthesis of the methyl *N*-Boc-6-

Scheme 4. Synthesis of the amide terminus and permethylated peptide backbone





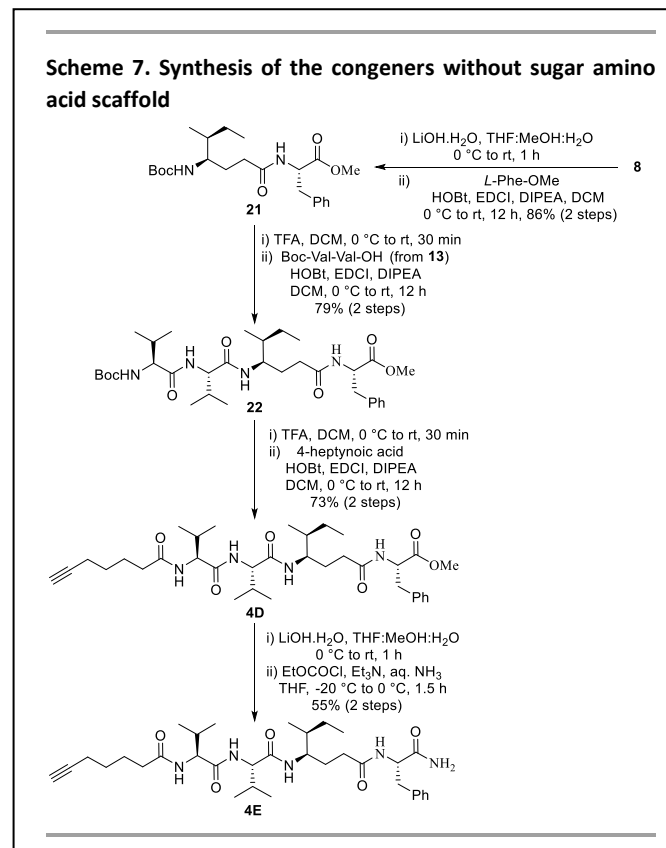
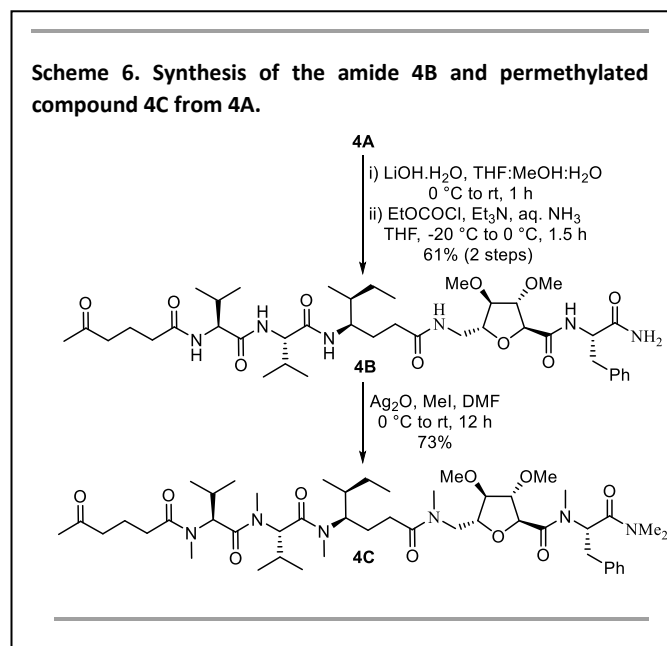
amino-2,5-anhydro-3,4-di-*O*-methyl-6-deoxy-*D*-mannonate, Boc-MAA(Me)₂-OMe (**9**), was accomplished in 11 steps using *D*-mannitol as the starting material following the reported procedure.^{11c,d} MAA(Me)₂ was used to replace the Val-Ala spacer segment of almiramides.

Synthesis of the linear tetrapeptide 14. Having prepared the unnatural monomeric units required for the synthesis of the analogues, the stage was set for the synthesis of the target peptides. The linear tetrapeptide **14** was synthesized by coupling MAA (**9**) with L-Phe and then attaching Val-Val¹⁷ to the *N*-terminus of MAA-Phe following linear peptide coupling method as depicted in the Scheme 2. Standard solution phase peptide synthesis method using 1-ethyl-3-(3-dimethylamino)propyl)carbodiimide hydrochloride (EDCI) and 1-hydroxybenzotriazole (HOBt) as coupling agents, DIPEA as base and DCM as solvent was followed to build these peptides. While the Boc group was used for *N*-protection, the *C*-terminal was protected as methyl esters. Deprotection of the former was carried out with trifluoroacetic acid (TFA) in DCM to furnish the TFA salt and saponification of the methyl ester was achieved with LiOH.H₂O in THF/MeOH/H₂O (3:1:1) to give the

corresponding carboxylic acids, which were directly used after aqueous work-up for the next peptide coupling reaction without further purification or characterization.

Incorporation of the lipophilic side chains. Having successfully prepared the tetrapeptide **14** with *C*-terminal methyl ester, we turned our attention to incorporate the lipid side chains (chain length is variable and ranges from 6 to 10 carbons, Figure 2) to create the structural diversity at the *N*-terminus.

The tetrapeptide **14** upon treatment with TFA in DCM gave the corresponding TFA salt **15** (Scheme 3). Coupling of **15** with various acids having the lipophilic side chains under standard peptide coupling conditions by sequential addition of HOBt and EDCI followed by DIPEA in DCM gave the lipid-attached peptides with a general structure **16** as shown in Scheme 3 – comprising compounds **4F**, **4I**, **4L**, **4O**, **4R** and **4U**.



Synthesis of the primary amide C-terminus and the fully methylated peptide backbone. After the *N*-terminal lipid chain insertion, we next sought to prepare the C-terminal primary

analogues **18** (Scheme 4) with fully methylated backbones represented by **4H**, **4K**, **4N**, **4Q**, **4T** and **4W**.
View Article Online
DOI: 10.1039/C6OB02610A

Synthesis of 4A-C containing the γ -amino acid (AMH, **8) and MAA (**9**).** After that, we decided to undertake the synthesis of a small library of pentapeptides **4A-C**, containing both the γ -amino acid AMH (**8**) and δ -amino acid MAA (**9**), to access another type of structural diversity mainly focusing on the number of amino acids (i.e. five, same as in almiramides) instead of the total number of atoms in the linear peptidic chain. Compound **4A** was synthesized from the appropriate amino acid precursor as described in Scheme 5. Then it was converted to its amide **4B** and the permethylated compound **4C** as shown in Scheme 6.

To further optimize our library, the 2nd generation modification was aimed to devise analogues **4D-E** which were different from the others due to the absence of any SAA, to prove the viability of the SAA based scaffold in the design and activity (Scheme 7).

Biological evaluations: antileishmanial activities. After successful preparation of the compounds, we were next interested to identify new and potent antileishmanial leads from the library. For that, all the compounds were screened against *L. donovani*. Each candidate was evaluated for its *in vitro* activity against intra-macrophagic amastigotes and also evaluated for their cytotoxic properties over mammalian Vero cells (kidney fibroblast cells).

Gratifyingly, the compounds **4C**, **4E**, **4N**, **4Q**, **4T**, **4U** and **4W** exhibited moderate micromolar activity, having poor to moderate selectivity profiles, with IC₅₀ values ranging from 10.1 to 26.67 μ M (Table 1). A progressive enhancement of the activity was observed in the case of the compounds having the MAA scaffold. It was also observed that, overall variations in the functional groups at the C-terminus as well as at the *N*-terminus have significant effect on activity. Close investigation of the activity of each series of peptides revealed that the compounds which contained C-terminal primary amide derivatives were completely inactive as compared to the compounds containing either methyl ester or tertiary amide. This observation was contrasting with the biological data reported by Linington *et al.*^{8c,9} where the C-terminal methyl ester derivatives were largely inactive in the screen. The improvement in the present study might be due to the fact that the esters were better tolerated in our compounds and also, due to the less polarity, they had better membrane permeability as compared to the more polar amides. Importantly, our permethylated compounds displayed better activity presumably due to their increased membrane permeabilities. Although their selectivity profiles still remained moderate, they were comparable to that of the standard antileishmanial drug, miltefosine (last entry, Table 1). The permethylated compounds were also explored earlier by Linington *et al.*^{8c,9} and some of their analogues showed superior activity and cytotoxicity profiles.

Having confirmed the importance of the permethylated analogues, we next screened various permethylated derivatives with variable lipid chains and found that the

Table 1. Bioactivities of the synthetic analogues

Compound	Antiamastigote activity (IC ₅₀ , μ M) (MQ/amast. model)	Cytotoxicity on Vero cells (CC ₅₀ , μ M)	Selectivity Index* (CC ₅₀ / IC ₅₀)
4A	>100	295.47	<2.95
4B	>100	>400	4.0
4C	26.41	79.43	3.0
4D	>100	210.25	<2.10
4E	>25	125.21	<5.0
4F	92.18	>400	>4.33
4G	>100	>400	4.0
4H	56.48	79.51	1.40
4I	>100	>400	4.0
4J	>100	>400	4.0
4K	>100	>400	4.0
4L	60.67	>400	>6.59
4M	>100	>400	4.0
4N	26.67	24.07	0.90
4O	68.48	>400	5.84
4P	>100	>400	4.0
4Q	10.10	14.53	1.44
4R	>50	>400	8.0
4S	>100	>400	4.0
4T	10.92	58.35	5.34
4U	22.86	>400	>17.49
4V	>100	>400	4.0
4W	13.63	95.31	6.99
MF[†]	8.48	51.27	6.05

* Selectivity index (SI) is defined as the ratio of CC₅₀ on mammalian kidney fibroblast cells (Vero cell line) to IC₅₀ on *L. donovani* intracellular amastigotes. [†] MF (miltefosine) was used as a reference antileishmanial drug.

amide and its corresponding permethylated analogues as *N*-methylation of peptides is known to lead to improved membrane permeability, pharmacokinetic properties and better biological activities.¹⁸ Preparation of these compounds is shown in Scheme 4. Saponification of **16** with LiOH.H₂O in THF/MeOH/H₂O (3:1:1) was carried out and the resulting carboxylic acids were converted to their amides by treatment with aq. NH₃ in presence of ethyl chloroformate and Et₃N to furnish C-terminus amides with general structure **17** (Scheme 4), representing **4G**, **4J**, **4M**, **4P**, **4S** and **4V**.¹⁹ Next, permethylation using Ag₂O and MeI in DMF generated the

compounds **4D**, **4E**, **4I**, **4J** and **4K** were inactive, indicating the intolerance of the alkyne moiety at the peptide terminus. Further, it is to be noted here that the compounds with saturated alkyl chain **4Q** and the olefin terminus **4T** showed comparable activity with better selectivity for the later, in conflict with the earlier result⁹ which endorsed the

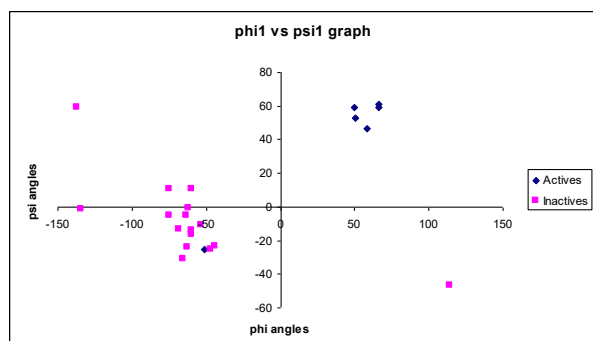


Figure 3. Conformational preferences of the torsional angles. Phi-1 and psi-1 are the dihedral angles of the first residue in the peptidomimetic compounds.

requirement of an unsaturated terminus on the side chain over saturated one for better activity. We next explored the importance of the length of the lipid chain which was varied from 6 to 10 carbons and the results suggested that the bioactivity increases with the increase in the chain length. Further, increment of the total peptide length by incorporating one extra amino acid residue that led to compounds **4A-C** showed no significant improvement in activity.

Computational approach to Structure-Activity Relationship (SAR) studies. The encouraging results of the analogues prompted us to explore SAR analysis to find out the role of each of the components of the peptide backbone.

Molecules were drawn and minimized in MOE²¹ followed by partial charge calculation using AMBER99.²² Structures were subsequently subjected to molecular dynamics simulation at 300 K and AMBER99 force field in vacuum with 100 ps of equilibrium run followed by production run for 500 ps. Resulting structures were analysed in Chimera.²³

Peptidomimetics adopt specific conformation in solution to interact with the corresponding target proteins. In this work, as the target was not known, SAR studies were performed using molecular dynamics simulations on the given set of peptidomimetic compounds to examine if there was any conformational pattern that could be correlated to their antileishmanial activities. From three dimensional arrangements of the atoms in these molecules, a clear conformational preference of the torsional angles (phi and psi angles) around first peptide bond for the active molecules over the inactive ones was observed (Figure 3). Peptidomimetic molecules with both positive phi and psi values for the first residue were found to be relatively more active while inactive molecules could have negative values for either or both phi and psi values for the first residue. These differences demonstrate the H-bond forming ability of the first residue in each molecule. Therefore, preferred conformation of the molecules can be prioritized using phi-psi angles to establish the blueprint for biological activity. Moreover, profound effect of *N*-methylation of peptide bonds can be distinguished clearly from the visual analysis of the molecular structures. However, from the listings of phi and psi values for the compounds (see Table S1, Supporting Information), it is seen that compound **4U**, which is not *N*-methylated and, therefore, having negative phi and psi values, is still considerably active. Activity of this compound could be attributed to the larger exposed non-polar surface area due to the presence of the phenyl ring containing long aliphatic chain at *N*-terminus as discussed below.

Observation of the three dimensional structures of the compounds (Figure 4) highlighted that the amide proton containing

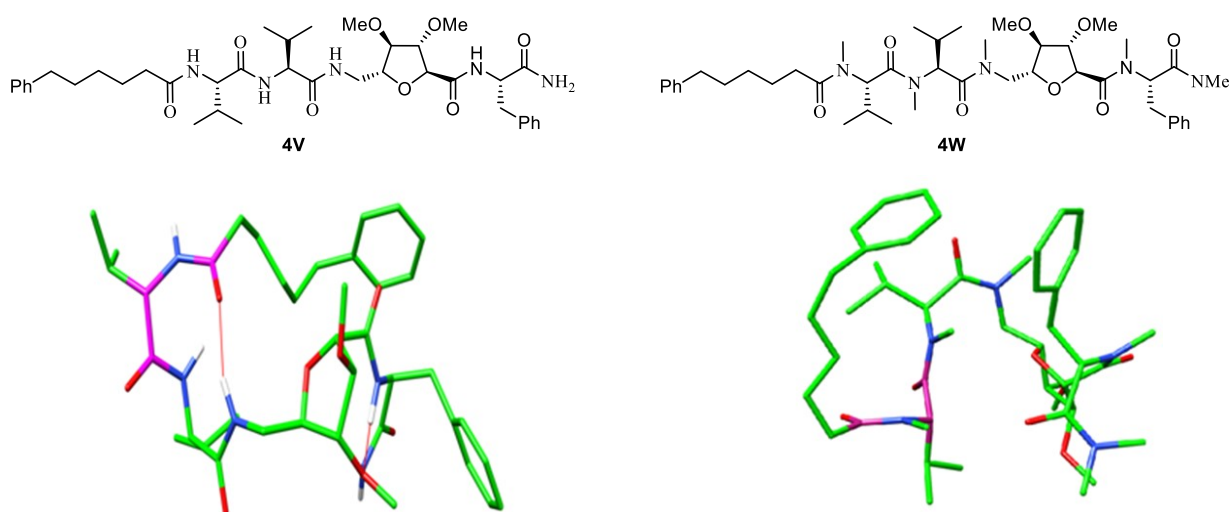


Figure 4. Effect of the H-bonding on the structural changes in the peptides. Unlike active molecules (**4W**), inactive molecules (**4V**) are characterized by the presence of β -turn due to the formation of H-bond.

molecules form the hydrogen bond between the carbonyl oxygen of the first acyl residue and amide proton of the third residue which adopt a particular tight 10-membered β -turn. This results into reduced flexibility of the *N*-terminal hydrophobic chains which turn around the backbone leading to the disruption of the coiled secondary structure and also in the reduction of the hydrophobic surface area. Moreover, beside H-bond, hydrophobicity may also be playing the role of one of the determining factors for the activity. Long hydrophobic chain at *N*-terminus is probably more favorable for the antileishmanial activity. As obvious from the activity data, **4K** and **4H** have relatively poor activity although having *N*-methylated amide but low hydrophobic surface area. Whereas, among the *N*-protonated peptides, **4U** and **4O** (to a lesser extent) were found to be somewhat active due to the presence of long chain hydrophobic groups. It seems that the presence of long aliphatic/aromatic groups at the *N*-terminal end causes steric clashes with the *C*-terminal hydrophobic groups and, therefore, forces them to turn away from the backbone, leading to an increase in the total hydrophobic surface area. Additionally, presence of polar groups like $-\text{NH}_2$ group at the other *N*-terminal end also reduces the activity to some extent as evident from compounds **4P** and **4V** in comparison to **4O** and **4U**, respectively, having the same structure except the *C*-terminal groups.

Conformational analysis by NMR. Solution conformational analyses on selected peptides **4P**, **4Q**, **4V** and **4W** were undertaken in an attempt to decipher the underlying structural implications that might have led to much improved biological activities found in the permethylated analogues **4Q** and **4W** over their inactive unmethylated counterparts **4P** and **4V**, respectively. NMR studies were carried out in $\text{DMSO}-d_6$ with 5–10 mM concentration of the samples. For peptides **4P** and **4V**, single set of resonance observed in the proton spectrum suggested that these peptides exist in single conformation in the NMR time scale. The variable temperature (VT) study carried out in $\text{DMSO}-d_6$, suggested minimal $\Delta\delta/\Delta T$ value for PheNH supporting its participation in hydrogen bonding. Wide dispersion of the amide protons suggested stable secondary structure for these peptides, and further the characteristic nOes $\text{PheNH} \leftrightarrow \text{MaaC}\delta\text{H}$, $\text{PheNH} \leftrightarrow \text{MaaC}\epsilon\text{H}$ (see Figure S7 in supporting information) and minimal $\Delta\delta/\Delta T$ value for PheNH suggest a 10-membered β -turn structure involving PheNH and ^2Val carbonyl, in contrast to the 10-membered β -turn structure involving MAANH and *C*-terminus acyl carbonyl theoretically observed in SAR analysis.

The permethylated peptides **4Q** and **4W** that showed the best antileishmanial activities, exhibited either broad peaks or multiple peaks in $\text{DMSO}-d_6$ which may be as a result of multiple conformations that are either in the intermediate or slow exchange regime in the NMR time scale. The chemical shift assignments for the major conformer were made and are tabulated in the supporting information. Though there may be lack of H-bonding as because of the absence of amide protons, yet the turn structures were evident among these peptides as we have seen a characteristic nOe correlation observed from the NMR of the Phe

residue and $\text{MAAC}\delta\text{H}$, suggesting that the bent turn structure may also be there as seen in their counterparts. DOI: 10.1039/C6OB02610A

Molecular dynamics simulation based on NMR data. Energy minimization and simulated molecular dynamics (MD) calculations were performed on Discovery studio 3.0 version,^{24a} using CHARMM force field^{24b} with default parameters throughout the simulation with the aid of distance dependent dielectric constant with $\epsilon = 46.7$ (dielectric constant for DMSO). Distance restraints used in the MD were calculated from the volume integrals of the cross peaks in the ROESY spectra by categorizing them as strong, medium and weak peaks based on their volume integrals. Force constants of 10 K cal/ \AA , 5 K cal/ \AA were employed for distance and torsional restraints respectively. Minimization was done with steepest descent algorithm followed by conjugate gradient methods for maximum 1000 iterations each iterations or RMS deviation of 0.001 Kcal/mol, whichever was earlier. The molecules were initially equilibrated for 5 pS and then subjected to 1 nS production run. Starting from 50 K, they were heated to 300 K in five steps, increasing the temperature 50 K at each step. 20 structures were stored from the production run and were again energy minimized with the above-mentioned protocol. Superposition was done on to the average structure of these minimized structures. The superimposed 10 energy minimized structures of **4P** and **4V** are shown in Figure 5. The structures of **4P** and **4V** based on NMR data, although appear different than those derived computationally (Figure 4), bear a commonality in brining the *C*-terminus close to the lipophilic end of the fatty acid chain leading to a more condensed hydrophobic surface.

Conclusions

In conclusion, inspired by the interesting biological activities of almiramides, we have synthesized a small library of 23 linear lipopeptides by incorporating a mannose-derived furanoid

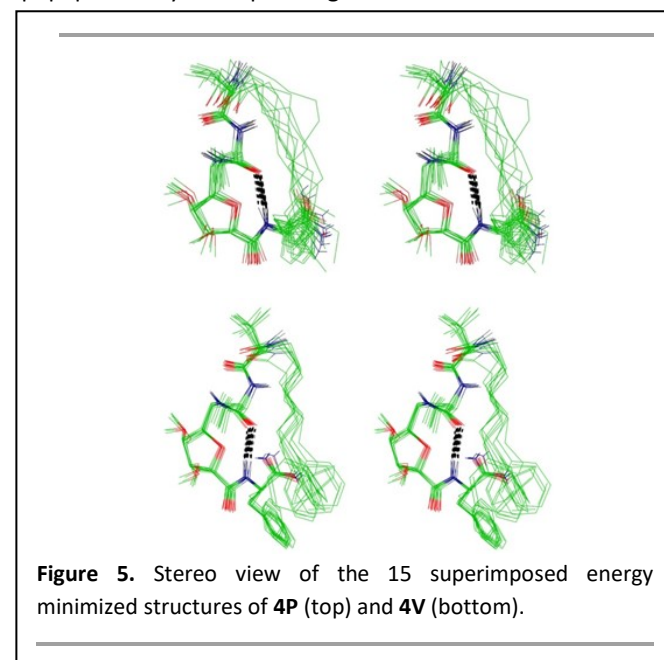


Figure 5. Stereo view of the 15 superimposed energy minimized structures of **4P** (top) and **4V** (bottom).

sugar amino acid as a novel scaffold along with other building blocks and assessed them against intra-macrophagic amastigotes of *L. donovani*. A number of such compounds exhibited *in vitro* activity comparable to the other current antileishmanials. To the best of our knowledge, peptides with sugar amino acid based scaffolds and their antileishmanial activities have never been reported to date. The SAR and NMR studies revealed that among all the synthesized compounds, the MAA-containing permethylated analogues having longer hydrophobic chains at the *N*-terminus were more active than their unmethylated counterparts possibly due to the improved cell permeability of the former resulting from their condensed hydrophobic surface. Hence, the SAA based scaffolds can serve as a useful building block for further antileishmanial lead development. Especially explorations with the other stereoisomeric variants of this multifunctional hybrid molecule, their incorporation into the lead sequences found in the present study and evaluation of their biological profiles could lead to the prospective antileishmanials of tomorrow.

Experimental Section

General Experimental Details: All the reactions were carried out under an inert atmosphere in oven-dried glassware using dry solvents, unless otherwise stated. All chemicals purchased from commercial suppliers were used as received unless otherwise stated. Reactions and chromatography fractions were monitored by Merck silica gel 60 F-254 glass TLC plates and visualized using UV light, 7% ethanolic phosphomolybdic acid-heat, 2.5% ethanolic anisaldehyde (with 1% AcOH and 3.3% conc. H_2SO_4), ninhydrin or chlorine/*o*-tolidine-heat as developing agents. Flash column chromatography was performed with 100-200 mesh silica gel and yields refer to chromatographically and spectroscopically pure compounds.

All NMR spectra were recorded in CDCl_3 or in $\text{DMSO}-d_6$ on a 300, 400 and 500 MHz instruments at 300 K and are calibrated to residual solvent peaks (CHCl_3 7.26 ppm and 77.0 ppm, DMSO 2.50 ppm and 40.0 ppm). Multiplicities are abbreviated as: s = singlet; d = doublet; t = triplet; q = quartet; m = multiplet. All IR data were recorded as neat liquid or KBr pellets using a Perkin Elmer's RX I FTIR spectrophotometer. Mass spectra were obtained under electron spray ionisation (ESI) and HRMS spectra were taken with a 3000 mass spectrometer using Waters Agilent 6520-Q-ToFMS/MS system and JEOL-AccuTOF JMS-T100 LC. RP-HPLC was performed on a Waters HPLC system and Shimadzu's ISO 9001 HPLC system (model no. LC-20AD) equipped with a 5 μ SunFire C18 column (4.6 \times 250 mm) and 5 μ Shimadzu's C18 column (4.6 \times 250 mm) respectively in combination with eluants A (H_2O) and B (MeCN) with flow rate: 0.8 mL/min and photodiode array detector setting of λ = 210-254 nm.

Experimental Procedures and Characterization Data:

Preparation of 8: Compounds **6** and **7** were synthesized according to the literature procedures¹⁶. To a solution of the ester **7** (1.0 g,

3.5 mmol) in EtOH (10 mL), 10% Pd/C (164 mg) was added and the mixture was hydrogenated at room temperature using a H_2 -filled balloon for 2 h. The solution was then filtered through a short pad of Celite and the filter cake was washed with EtOAc. The filtrate and washings were combined and concentrated in *vacuo*. Flash column chromatography (Silica gel, 8% EtOAc in Hexane) furnished **8** (984 mg, 98%) as colorless oil.

R_f = 0.45 (Silica gel, 15% EtOAc in Hexane); ^1H NMR (400 MHz, CDCl_3): δ 4.35 (d, J = 9.6 Hz, 1H), 4.11 (q, J = 7.0 Hz, 2H), 3.48 (m, 1H), 2.33 (t, J = 7.6 Hz, 2H), 1.85 – 1.75 (m, 1H), 1.60 – 1.35 (m, 12H), 1.24 (t, J = 7.1 Hz, 3H), 1.15 – 1.03 (m, 1H), 0.95 – 0.80 (m, 6H); ^{13}C NMR (100 MHz, CDCl_3): δ 173.84, 155.79, 78.95, 60.38, 54.43, 39.25, 31.44, 28.37, 26.47, 25.25, 14.89, 14.19, 11.74; IR ν_{max} (neat, cm^{-1}): 3366, 2968, 2930, 2876, 1711, 1597, 1521, 1453, 1368, 1249, 1174, 1019; MS (ESIMS/[M+Na] $^+$): m/z (%) 310; HRMS (ESI/[M+Na] $^+$): Calcd for $\text{C}_{15}\text{H}_{29}\text{NO}_4\text{Na}^+$: 310.1989, found 310.1987.

General Procedure for the Saponification of Ester: To a solution of compound in THF/MeOH/ H_2O (3:1:1, 3 mL/mmol) at 0 $^\circ\text{C}$ was added LiOH. $\cdot\text{H}_2\text{O}$ (3 eq) and the mixture was stirred at room temperature for 1 h. The mixture was then acidified to pH 2 with 1N HCl at 0 $^\circ\text{C}$. The reaction mixture was extracted with EtOAc, washed with water and brine, dried (Na_2SO_4), filtered and concentrated in *vacuo* to obtain the corresponding acid. The crude acid was used directly in the next step without further purification.

General Procedure for Deprotection of *N*-Boc Group: To the compound in DCM (3 mL/mmol) at 0 $^\circ\text{C}$, was added trifluoroacetic acid (TFA; 1 mL/mmol) and the mixture was stirred for 30 min at room temperature. The reaction mixture was then concentrated in *vacuo*, followed by azeotroping with DCM for 3 times to obtain the trifluoroacetate salt which was directly used in the next step.

General Procedure for Peptide Coupling: To a stirring solution of the acid in DCM (3 mL/mmol) or DMF (3 mL/mmol) at 0 $^\circ\text{C}$ were sequentially added 1-hydroxybenzotriazole (HOBt, 1.5 eq) and 1-ethyl-3-(3-(dimethylamino)-propyl)carbodiimide hydrochloride (EDCI, 1.5 eq). After 10 min, the previously prepared trifluoroacetate salt was cannulated into the reaction mixture followed by the addition of DIPEA (5 eq). The reaction mixture was brought to room temperature and continuously stirred for 12 h. The reaction mixture was then extracted with EtOAc and washed with 1N HCl, saturated aqueous NaHCO_3 solution, water and brine, dried (Na_2SO_4), filtered and concentrated in *vacuo*. Purification by column chromatography (100-200 mesh silica gel, 0.8-1.5% MeOH in chloroform as eluant for compounds **4A**, **4D**, **4F**, **4I**, **4L**, **4O**, **4R** and **4U**) afforded the coupling product.

Data for 11: Scale of reaction 1.0 g, 3.13 mmol; yield 1.21 g, 83% (Purification by column chromatography in 100-200 mesh silica gel, 35% EtOAc in hexane as eluant).

R_f = 0.50 (Silica gel, 70% EtOAc in Hexane); ^1H NMR (400 MHz, CDCl_3): δ 7.3 – 7.2 (m, 3H), 7.16 – 7.11 (m, 2H), 7.06 (d, J = 8.2 Hz, 1H), 4.94 (m, 1H), 4.89 – 4.83 (m, 1H), 4.41 (d, J = 1.5 Hz, 1H), 4.06 (t, J = 1.4 Hz, 1H), 4.04 – 3.98 (m, 1H), 3.69 (s, 3H), 3.57 (dd, J = 2.2,

1.5 Hz, 1H), 3.41 (s, 3H), 3.38 – 3.31 (m, 1H), 3.29 (s, 3H), 3.27 – 3.19 (m, 1H), 3.13 – 3.01 (m, 2H), 1.45 (s, 9H); ¹³C NMR (100 MHz, CDCl₃): δ 171.48, 169.86, 155.92, 135.67, 129.32, 128.55, 127.15, 86.88, 85.62, 83.89, 82.76, 79.39, 77.20, 57.33, 52.56, 52.27, 42.24, 38.03, 28.35; IR ν_{max} (neat, cm⁻¹): 3405, 3350, 2977, 2933, 2828, 1744, 1710, 1519, 1447, 1365, 1274, 1251, 1172, 1112, 1088, 1020; MS (ESIMS/[M+Na]⁺): *m/z*(%) 489; HRMS (ESI/[M+Na]⁺): Calcd for C₂₃H₃₄N₂O₈Na⁺: 489.2207, found 489.2315.

Data for 14: Scale of reaction 1.2 g, 2.57 mmol; yield 1.33 g, 78% (Purification by column chromatography in 100-200 mesh silica gel, 2% MeOH in chloroform as eluant).

R_f = 0.52 (Silica gel, 5% MeOH in CHCl₃); ¹H NMR (400 MHz, CDCl₃): δ 7.29 – 7.20 (m, 3H), 7.15 – 7.08 (m, 3H), 6.83 (t, *J* = 5.7 Hz, 1H), 6.64 (d, *J* = 8.5 Hz, 1H), 5.16 (d, *J* = 7.2 Hz, 1H), 4.89 – 4.82 (m, 1H), 4.42 (bs, 1H), 4.26 (dd, *J* = 8.2, 6.3 Hz, 1H), 4.06 (bs, 2H), 3.89 (t, *J* = 6.6 Hz, 1H), 3.68 (s, 3H), 3.61 (m, 1H), 3.43 (m, 5H), 3.26 (s, 3H), 3.13 – 3.01 (m, 2H), 2.26 – 2.16 (m, 1H), 2.14 – 2.07 (m, 1H), 1.42 (s, 9H), 0.96 – 0.85 (m, 12H); ¹³C NMR (100 MHz, CDCl₃): δ 171.78, 171.43, 171.08, 169.77, 156.10, 135.68, 129.29, 128.50, 127.10, 86.87, 85.71, 83.07, 82.59, 80.21, 60.51, 58.47, 57.36, 57.26, 52.61, 52.26, 41.04, 37.98, 28.20, 19.32, 19.29, 17.79, 17.59; IR ν_{max} (neat, cm⁻¹): 3313, 2961, 2928, 1648, 1566, 1518, 1443, 1365, 1290, 1219, 1154, 1086, 1018; MS (ESIMS/[M+Na]⁺): *m/z*(%) 687; HRMS (ESI/[M+Na]⁺): Calcd for C₃₃H₅₂N₄O₁₀Na⁺: 687.3575, found 687.3581.

Data for 19: Scale of reaction 400 mg, 0.86 mmol; yield 422 mg, 81% (Purification by column chromatography in 100-200 mesh silica gel, 50% EtOAc in hexane as eluant).

R_f = 0.52 (Silica gel, 80% EtOAc in Hexane); ¹H NMR (400 MHz, CDCl₃): δ 7.29 – 7.19 (m, 3H), 7.15 – 7.11 (m, 2H), 7.08 (d, *J* = 8.2 Hz, 1H), 6.45 (t, *J* = 5.5 Hz, 1H), 4.89 – 4.83 (m, 1H), 4.48 (d, *J* = 9.9 Hz, 1H), 4.43 (bs, 1H), 4.09 – 4.04 (m, 2H), 3.69 (s, 3H), 3.63 (bs, 1H), 3.52 – 3.35 (m, 6H), 3.28 (s, 3H), 3.13 – 3.00 (m, 2H), 2.44 – 2.10 (m, 3H), 1.89 – 1.78 (m, 1H), 1.60 – 1.36 (m, 11H), 1.14 – 1.03 (m, 1H), 0.90 – 0.83 (m, 6H); ¹³C NMR (100 MHz, CDCl₃): δ 173.29, 171.45, 169.79, 156.34, 135.65, 129.31, 128.50, 127.11, 86.71, 85.51, 83.71, 82.82, 79.15, 57.31, 57.25, 54.30, 52.58, 52.25, 41.05, 39.29, 38.01, 33.65, 28.35, 27.87, 25.22, 15.00, 11.72; IR ν_{max} (neat, cm⁻¹): 3335, 2962, 2928, 1744, 1666, 1524, 1449, 1366, 1219, 1171, 1111, 1018; MS (ESIMS/[M+Na]⁺): *m/z*(%) 630; HRMS (ESI/[M+Na]⁺): Calcd for C₃₁H₄₉N₃O₉Na⁺: 630.3361, found 630.3367.

Data for 20: Scale of reaction 410 mg, 0.65 mmol; yield 398 mg, 76% (Purification by column chromatography in 100-200 mesh silica gel, 2% MeOH in chloroform as eluant).

R_f = 0.49 (Silica gel, 8% MeOH in CHCl₃); ¹H NMR (400 MHz, CDCl₃): δ 7.28 – 7.17 (m, 4H), 7.16 – 7.10 (m, 2H), 6.91 (t, *J* = 6.1 Hz, 1H), 6.73 – 6.61 (m, 2H), 5.23 (d, *J* = 5.2 Hz, 1H), 4.88 – 4.80 (m, 1H), 4.40 (bs, 1H), 4.20 – 4.13 (m, 1H), 4.07 – 3.98 (m, 2H), 3.84 (t, *J* = 5.2 Hz, 1H), 3.80 – 3.72 (m, 1H), 3.66 (s, 3H), 3.64 – 3.60 (bs, 1H), 3.42 – 3.36 (m, 5H), 3.25 (s, 3H), 3.05 (d, *J* = 5.7 Hz, 2H), 2.40 – 2.06 (m, 4H), 2.01 – 1.87 (m, 1H), 1.63 – 1.34 (m, 11H), 1.14 – 1.01 (m, 2H), 0.99 – 0.76 (m, 18H); ¹³C NMR (100 MHz, CDCl₃): δ 173.51, 171.96, 171.57, 170.86, 170.12, 156.54, 135.77, 129.22, 128.47, 127.00, 87.11, 85.52, 83.37, 82.69, 80.64, 61.56, 59.45, 57.28, 57.14, 52.96,

52.61, 52.17, 41.10, 38.57, 37.92, 33.18, 29.58, 28.17, 27.25, 25.56, 19.67, 19.22, 17.65, 17.24, 14.96, 11.39; ¹H NMR (400 MHz, DMSO-*d*₆): δ 8.01 (d, *J* = 8.4 Hz, 1H), 7.91 (t, *J* = 5.7 Hz, 1H), 7.69 – 7.60 (m, 2H), 7.27 – 7.17 (m, 5H), 6.82 (d, *J* = 8.9 Hz, 1H), 4.58 – 4.52 (m, 1H), 4.29 (d, *J* = 2.2 Hz, 1H), 4.17 – 4.12 (m, 1H), 3.90 – 3.85 (m, 1H), 3.81 – 3.74 (m, 2H), 3.63 (s, 3H), 3.61 – 3.56 (m, 2H), 3.27 (s, 3H), 3.24 – 3.17 (m, 2H), 3.14 (s, 3H), 3.05 – 3.00 (m, 2H), 2.17 – 1.87 (m, 4H), 1.72 – 1.62 (m, 1H), 1.55 – 1.34 (m, 11H), 1.13 – 0.94 (m, 2H), 0.87 – 0.76 (m, 18H); ¹³C NMR (100 MHz, DMSO-*d*₆): δ 172.72, 172.09, 171.63, 170.97, 170.41, 155.91, 137.59, 129.61, 128.71, 126.99, 88.18, 85.66, 82.49, 82.40, 78.49, 60.57, 58.34, 57.30, 57.09, 53.33, 52.66, 52.52, 40.87, 38.49, 36.79, 32.91, 30.55, 28.64, 26.75, 25.40, 19.89, 19.69, 18.75, 18.63, 15.43, 11.93.

IR ν_{max} (neat, cm⁻¹): 3403, 3326, 3272, 2926, 1639, 1522, 1449, 1368, 1219, 1019; MS (ESIMS/[M+Na]⁺): *m/z*(%) 828; HRMS (ESI/[M+Na]⁺): Calcd for C₄₁H₆₇N₅O₁₁Na⁺: 828.4729, found 828.4737. HPLC data: Linear gradient 50→90% B in 10 mins, total run 20 mins, *t_R* = 12.425 min, 80% purity.

Data for 4A: Scale of reaction 390 mg, 0.48 mmol; yield 328 mg, 83%.

R_f = 0.51 (Silica gel, 5% MeOH in CHCl₃); ¹H NMR (300 MHz, CDCl₃): δ 7.37 – 7.07 (m, 7H), 7.06 – 6.76 (m, 3H), 4.94 – 4.81 (m, 1H), 4.63 – 4.48 (m, 1H), 4.41 (bs, 1H), 4.37 – 4.11 (m, 2H), 4.10 – 3.96 (m, 2H), 3.87 – 3.74 (m, 1H), 3.69 (s, 3H), 3.64 – 3.55 (m, 1H), 3.47 – 3.35 (m, 5H), 3.32 – 3.24 (m, 3H), 3.07 (d, *J* = 5.6 Hz, 2H), 2.48 (t, *J* = 6.7 Hz, 2H), 2.34 – 2.08 (m, 9H), 1.96 – 1.82 (m, 4H), 1.57 – 1.37 (m, 2H), 1.03 – 0.82 (m, 18H); ¹³C NMR (75 MHz, CDCl₃): δ 208.49, 173.79, 173.37, 172.85, 171.72, 171.63, 171.44, 169.99, 135.83, 129.25, 128.45, 127.01, 87.19, 85.93, 83.29, 82.73, 57.34, 57.15, 52.65, 52.22, 42.48, 41.07, 39.04, 37.94, 34.89, 31.84, 29.80, 29.61, 25.47, 22.60, 19.88, 19.39, 18.97, 18.69, 18.28, 14.92, 14.03, 11.59; ¹H NMR (400 MHz, DMSO-*d*₆): δ 8.01 (d, *J* = 8.3 Hz, 1H), 7.94 – 7.83 (m, 2H), 7.72 (d, *J* = 9.0 Hz, 1H), 7.59 (d, *J* = 8.9 Hz, 1H), 7.28 – 7.17 (m, 5H), 4.59 – 4.52 (m, 1H), 4.29 (d, *J* = 2.2 Hz, 1H), 4.21 – 4.07 (m, 2H), 3.92 – 3.84 (m, 1H), 3.76 (t, *J* = 1.9 Hz, 1H), 3.63 (s, 3H), 3.61 – 3.55 (m, 2H), 3.27 (s, 3H), 3.24 – 3.16 (m, 2H), 3.14 (s, 3H), 3.07 – 3.00 (m, 2H), 2.39 (t, *J* = 7.3 Hz, 2H), 2.17 – 2.09 (m, 3H), 2.05 (s, 3H), 1.97 – 1.88 (m, 2H), 1.70 – 1.61 (m, 2H), 1.55 – 1.31 (m, 4H), 1.10 – 0.99 (m, 2H), 0.88 – 0.76 (m, 18H); ¹³C NMR (100 MHz, DMSO-*d*₆): δ 208.59, 172.72, 172.35, 172.06, 171.40, 170.97, 170.39, 137.58, 129.59, 128.69, 126.97, 88.17, 85.65, 82.49, 82.39, 58.62, 58.28, 57.29, 57.07, 53.31, 52.65, 52.49, 42.44, 40.85, 38.47, 36.79, 34.65, 30.88, 30.58, 30.19, 25.31, 20.09, 19.85, 19.63, 18.70, 18.67, 15.46, 11.90; IR ν_{max} (neat, cm⁻¹): 3277, 2959, 2925, 1633, 1545, 1451, 1219, 1114, 1018; MS (ESIMS/[M+H]⁺): *m/z*(%) 818; HRMS (ESI/[M+H]⁺): Calcd for C₄₂H₆₈N₅O₁₁⁺: 818.4910, found 818.4900. HPLC data: Linear gradient 50→90% B in 10 mins, total run 20 mins, *t_R* = 7.863 min, 89% purity.

Data for 21: Scale of reaction 250 mg, 0.87 mmol; yield 314 mg, 86% (Purification by column chromatography in 100-200 mesh silica gel, 25% EtOAc in hexane as eluant).

R_f = 0.6 (Silica gel, 60% EtOAc in Hexane); ¹H NMR (400 MHz, CDCl₃): δ 7.31 – 7.20 (m, 3H), 7.19 – 7.14 (m, 2H), 6.86 (d, *J* = 7.1 Hz, 1H), 4.83 – 4.74 (m, 1H), 4.46 (d, *J* = 9.8 Hz, 1H), 3.72 (s, 3H), 3.67 –

3.57 (m, 1H), 3.16 (dd, $J = 13.9$, 5.3 Hz, 1H), 3.05 (dd, $J = 13.9$, 7.5 Hz, 1H), 2.25 – 2.12 (m, 2H), 1.86 – 1.70 (m, 2H), 1.55 – 1.39 (m, 11H), 1.16 – 1.02 (m, 1H), 0.94 – 0.82 (m, 6H); ^{13}C NMR (100 MHz, CDCl_3): δ 173.04, 172.21, 156.59, 136.29, 129.21, 128.47, 126.94, 79.29, 54.07, 53.63, 52.21, 39.26, 37.67, 33.28, 28.37, 28.32, 25.22, 15.08, 11.71; IR ν_{max} (neat, cm^{-1}): 3310, 2963, 2927, 2874, 1747, 1681, 1656, 1529, 1449, 1365, 1249, 1217, 1171, 1018; MS (ESIMS/[M+Na] $^+$): m/z (%) 443; HRMS (ESI/[M+H] $^+$): Calcd for $\text{C}_{23}\text{H}_{37}\text{N}_2\text{O}_5^+$: 421.2697, found 421.2692.

Data for 22: Scale of reaction 300 mg, 0.71 mmol; yield 349 mg, 79% (Purification by column chromatography in 100-200 mesh silica gel, 1.5% MeOH in chloroform as eluant).

$R_f = 0.4$ (Silica gel, 5% MeOH in CHCl_3); ^1H NMR (400 MHz, CDCl_3): δ 7.29 – 7.09 (m, 6H), 6.64 – 6.49 (m, 2H), 5.04 (d, $J = 5.6$ Hz, 1H), 4.82 – 4.75 (m, 1H), 4.21 – 4.12 (m, 1H), 3.81 – 3.66 (m, 5H), 3.16 (dd, $J = 13.8$, 5.7 Hz, 1H), 3.03 (dd, $J = 13.8$, 7.4 Hz, 1H), 2.38 – 2.06 (m, 4H), 1.98 – 1.86 (m, 1H), 1.62 – 1.39 (m, 12H), 1.16 – 1.03 (m, 1H), 1.00 – 0.79 (m, 18H); ^{13}C NMR (100 MHz, CDCl_3): δ 173.17, 172.29, 171.85, 170.89, 156.39, 136.51, 129.26, 128.36, 126.75, 80.72, 60.98, 59.40, 53.55, 53.36, 52.15, 38.39, 37.74, 33.04, 29.85, 29.25, 28.21, 27.73, 25.62, 19.69, 19.31, 17.62, 17.37, 15.14, 11.29; IR ν_{max} (neat, cm^{-1}): 3280, 2962, 2929, 2873, 1750, 1689, 1641, 1547, 1523, 1371, 1220, 1171, 1018; MS (ESIMS/[M+Na] $^+$): m/z (%) 641; HRMS (ESI/[M+H] $^+$): Calcd for $\text{C}_{33}\text{H}_{55}\text{N}_4\text{O}_7^+$: 619.4066, found 619.4069.

Data for 4D: Scale of reaction 295 mg, 0.48 mmol; yield 218 mg, 73%.

$R_f = 0.6$ (Silica gel, 10% MeOH in CHCl_3); ^1H NMR (300 MHz, $\text{DMSO}-d_6$): δ 8.21 (d, $J = 7.8$ Hz, 1H), 7.90 – 7.81 (m, 1H), 7.79 – 7.63 (m, 1H), 7.59 – 7.47 (m, 1H), 7.31 – 7.16 (m, 5H), 4.49 – 4.37 (m, 1H), 4.22 – 4.04 (m, 2H), 3.59 (s, 3H), 3.01 (dd, $J = 13.7$, 5.4 Hz, 1H), 2.86 (dd, $J = 13.7$, 9.5 Hz, 1H), 2.75 – 2.69 (m, 1H), 2.25 – 2.08 (m, 5H), 2.05 – 1.85 (m, 4H), 1.63 – 1.49 (m, 3H), 1.49 – 1.32 (m, 5H), 1.09 – 0.93 (m, 1H), 0.89 – 0.72 (m, 18H); ^{13}C NMR (75 MHz, $\text{DMSO}-d_6$): δ 172.62, 172.46, 171.39, 170.99, 137.77, 129.49, 128.61, 126.92, 84.79, 71.52, 58.65, 58.23, 53.99, 52.55, 52.21, 38.34, 37.11, 34.97, 32.58, 30.82, 30.60, 27.96, 25.23, 25.02, 19.80, 19.59, 18.71, 18.66, 17.91, 15.45, 11.83; IR ν_{max} (neat, cm^{-1}): 3279, 2925, 2868, 1740, 1635, 1542, 1454, 1223, 1019; MS (ESIMS/[M+H] $^+$): m/z (%) 627; HRMS (ESI/[M+Na] $^+$): Calcd for $\text{C}_{35}\text{H}_{54}\text{N}_4\text{O}_6\text{Na}^+$: 649.3935, found 649.3921. HPLC data: Linear gradient 50 \rightarrow 90% B in 10 mins, total run 25 mins, $t_R = 5.907$ min, 98% purity.

Data for 4F: Scale of reaction 300 mg, 0.45 mmol; yield 251 mg, 84%.

$R_f = 0.6$ (Silica gel, 10% MeOH in CHCl_3); ^1H NMR (400 MHz, CDCl_3): δ 7.28 – 7.18 (m, 4H), 7.16 – 7.10 (m, 3H), 6.93 – 6.83 (m, 1H), 6.66 – 6.56 (m, 1H), 4.89 – 4.82 (m, 1H), 4.44 – 4.37 (m, 2H), 4.28 – 4.22 (m, 1H), 4.07 – 4.02 (m, 2H), 3.69 (s, 3H), 3.60 – 3.58 (m, 1H), 3.45 – 3.38 (m, 5H), 3.26 (s, 3H), 3.09 – 3.05 (m, 2H), 2.25 – 2.17 (m, 3H), 2.17 – 1.95 (m, 2H), 1.67 – 1.54 (m, 4H), 1.33 – 1.25 (m, 4H), 0.95 – 0.82 (m, 12H); ^{13}C NMR (100 MHz, CDCl_3): δ 173.48, 171.89, 171.55, 171.29, 169.79, 135.77, 129.29, 128.49, 127.07, 86.86, 85.92, 83.17, 82.65, 58.83, 58.37, 57.39, 57.24, 52.67, 52.26, 41.01, 37.97, 31.36, 31.19, 30.60, 29.64, 25.48, 22.33, 19.23, 19.14, 18.36, 18.11, 13.88;

IR ν_{max} (neat, cm^{-1}): 3274, 2958, 2927, 1745, 1631, 1545, 1450, 1113, 1018; MS (ESIMS/[M+Na] $^+$): m/z (%) 685; HRMS (ESI/[M+Na] $^+$): Calcd for $\text{C}_{34}\text{H}_{54}\text{N}_4\text{O}_9\text{Na}^+$: 685.3783, found 685.3773. HPLC data: Linear gradient 50 \rightarrow 90% B in 10 mins, total run 20 mins, $t_R = 7.758$ min, 88% purity.

Data for 4I: Scale of reaction 135 mg, 0.18 mmol; yield 93 mg, 78%.

$R_f = 0.6$ (Silica gel, 6% MeOH in CHCl_3); ^1H NMR (400 MHz, CDCl_3): δ 7.28 – 7.19 (m, 4H), 7.17 – 7.10 (m, 3H), 6.95 – 6.82 (m, 1H), 6.80 – 6.61 (m, 1H), 4.90 – 4.82 (m, 1H), 4.50 – 4.36 (m, 2H), 4.26 (t, $J = 8.0$ Hz, 1H), 4.10 – 3.98 (m, 2H), 3.69 (s, 3H), 3.62 – 3.57 (m, 1H), 3.49 – 3.36 (m, 5H), 3.26 (s, 3H), 3.13 – 3.03 (m, 2H), 2.43 – 2.31 (m, 2H), 2.26 – 2.19 (m, 2H), 2.16 – 1.94 (m, 3H), 1.91 – 1.78 (m, 2H), 0.98 – 0.84 (m, 12H); ^{13}C NMR (100 MHz, CDCl_3): δ 172.52, 171.72, 171.57, 171.24, 169.77, 135.77, 129.30, 128.49, 127.09, 86.80, 85.96, 83.41, 83.19, 82.64, 69.21, 58.83, 58.38, 57.42, 57.28, 52.66, 52.30, 41.03, 37.97, 34.89, 31.28, 30.66, 24.22, 19.22, 19.13, 18.32, 18.17, 17.81; IR ν_{max} (neat, cm^{-1}): 3275, 2959, 2929, 1745, 1674, 1631, 1545, 1220, 1114, 1018; MS (ESIMS/[M+Na] $^+$): m/z (%) 681; HRMS (ESI/[M+Na] $^+$): Calcd for $\text{C}_{34}\text{H}_{50}\text{N}_4\text{O}_9\text{Na}^+$: 681.3470, found 681.3472. HPLC data: Isocratic (50%), total run 25 mins, $t_R = 7.910$ min, 92% purity.

Data for 4L: Scale of reaction 283 mg, 0.43 mmol; yield 209 mg, 71 %.

$R_f = 0.49$ (Silica gel, 6% MeOH in CHCl_3); ^1H NMR (400 MHz, CDCl_3): δ 7.29 – 7.19 (m, 3H), 7.16 – 7.02 (m, 4H), 6.86 – 6.75 (m, 1H), 6.58 – 6.45 (m, 1H), 4.89 – 4.83 (m, 1H), 4.44 – 4.35 (m, 2H), 4.28 – 4.21 (m, 1H), 4.08 – 4.00 (m, 2H), 3.69 (s, 3H), 3.60 – 3.57 (m, 1H), 3.50 – 3.34 (m, 5H), 3.27 (s, 3H), 3.12 – 3.03 (m, 2H), 2.25 – 2.19 (m, 1H), 2.17 – 2.08 (m, 1H), 2.06 – 1.99 (m, 2H), 1.66 – 1.56 (m, 2H), 1.31 – 1.22 (m, 8H), 0.94 – 0.83 (m, 15H); ^{13}C NMR (100 MHz, CDCl_3): δ 173.47, 171.79, 171.57, 171.17, 169.77, 135.77, 129.30, 128.50, 127.09, 86.85, 85.96, 83.16, 82.66, 58.79, 58.40, 57.41, 57.29, 52.68, 52.28, 41.05, 37.98, 36.58, 31.66, 31.15, 30.61, 29.19, 28.98, 25.81, 22.55, 19.25, 19.16, 18.32, 18.06, 14.01; IR ν_{max} (neat, cm^{-1}): 3276, 2957, 2927, 1745, 1675, 1631, 1544, 1453, 1223, 1111, 1018; MS (ESIMS/[M+H] $^+$): m/z (%) 691; HRMS (ESI/[M+Na] $^+$): Calcd for $\text{C}_{36}\text{H}_{58}\text{N}_4\text{O}_9\text{Na}^+$: 713.4096, found 713.4101. HPLC data: Linear gradient 50 \rightarrow 90% B in 10 mins, total run 30 mins, $t_R = 10.54$ min, 94% purity.

Data for 4O: Scale of reaction 300 mg, 0.45 mmol; yield 266 mg, 82 %.

$R_f = 0.6$ (Silica gel, 6% MeOH in CHCl_3); ^1H NMR (400 MHz, CDCl_3): δ 7.28 – 7.16 (m, 4H), 7.15 – 7.10 (m, 3H), 6.86 (t, $J = 5.2$ Hz, 1H), 6.61 (d, $J = 8.8$ Hz, 1H), 4.89 – 4.83 (m, 1H), 4.44 – 4.37 (m, 2H), 4.28 – 4.21 (m, 1H), 4.08 – 4.00 (m, 2H), 3.69 (s, 3H), 3.61 – 3.57 (m, 1H), 3.47 – 3.36 (m, 5H), 3.26 (s, 3H), 3.13 – 3.03 (m, 2H), 2.27 – 1.96 (m, 4H), 1.67 – 1.55 (m, 2H), 1.33 – 1.18 (m, 15H), 0.94 – 0.83 (m, 12H); ^{13}C NMR (100 MHz, CDCl_3): δ 173.50, 171.89, 171.55, 171.24, 169.77, 135.75, 129.30, 128.49, 127.09, 86.78, 85.91, 83.16, 82.63, 58.80, 58.35, 57.41, 57.28, 52.66, 52.29, 41.03, 37.97, 36.56, 31.81, 31.18, 30.59, 29.44, 29.34, 29.25, 29.23, 25.83, 22.61, 19.24, 19.15, 18.33, 18.09, 14.06; IR ν_{max} (neat, cm^{-1}): 3280, 2957, 2926, 1746, 1676, 1633, 1545, 1453, 1224, 1113, 1019; MS (ESIMS/[M+Na] $^+$): m/z (%) 741; HRMS (ESI/[M+Na] $^+$): Calcd for $\text{C}_{38}\text{H}_{62}\text{N}_4\text{O}_9\text{Na}^+$:

741.4409, found 741.4402. **HPLC data:** Linear gradient 50→90% B in 10 mins, total run 20 mins, t_R = 13.599 min, 96% purity.

Data for 4R: Scale of reaction 250 mg, 0.37 mmol; yield 197 mg, 73 %.

R_f = 0.5 (Silica gel, 5% MeOH in CHCl_3); $^1\text{H NMR}$ (400 MHz, CDCl_3): δ 7.28 – 7.21 (m, 3H), 7.16 – 7.10 (m, 3H), 7.05 – 6.96 (m, 1H), 6.79 – 6.71 (m, 1H), 6.49 – 6.42 (m, 1H), 5.84 – 5.72 (m, 1H), 5.01 – 4.83 (m, 3H), 4.43 – 4.40 (m, 1H), 4.39 – 4.34 (m, 1H), 4.26 – 4.21 (m, 1H), 4.07 – 4.01 (m, 2H), 3.69 (s, 3H), 3.59 – 3.56 (m, 1H), 3.52 – 3.34 (m, 5H), 3.27 (s, 3H), 3.13 – 3.03 (m, 2H), 2.24 – 1.95 (m, 4H), 1.66 – 1.56 (m, 2H), 1.39 – 1.23 (m, 10H), 0.95 – 0.86 (m, 12H); $^{13}\text{C NMR}$ (100 MHz, CDCl_3): δ 173.42, 171.76, 171.58, 171.13, 169.75, 139.02, 135.76, 129.31, 128.51, 127.11, 114.17, 86.83, 85.97, 83.16, 82.66, 58.78, 58.42, 57.42, 57.30, 52.67, 52.29, 41.07, 37.98, 36.57, 33.69, 31.13, 30.61, 29.18, 29.16, 28.92, 28.80, 25.77, 19.26, 19.17, 18.30, 18.03; **IR** ν_{max} (neat, cm^{-1}): 3278, 2958, 2926, 1746, 1675, 1632, 1545, 1448, 1222, 1114, 1018; **MS** (ESIMS/[M-1] $^+$): m/z (%) 715; **HRMS** (ESI/[M+Na] $^+$): Calcd for $\text{C}_{38}\text{H}_{60}\text{N}_4\text{O}_9\text{Na}^+$: 739.4252, found 739.4258. **HPLC data:** Linear gradient 50→90% B in 10 mins, total run 25 mins, t_R = 13.682 min, 93% purity.

Data for 4U: Scale of reaction 280 mg, 0.42 mmol; yield 261 mg, 84 %.

R_f = 0.6 (Silica gel, 3% MeOH in CHCl_3); $^1\text{H NMR}$ (400 MHz, CDCl_3): δ 7.28 – 7.21 (m, 6H), 7.18 – 7.11 (m, 6H), 6.89 – 6.82 (m, 1H), 6.56 (d, J = 8.6 Hz, 1H), 4.90 – 4.83 (m, 1H), 4.45 – 4.38 (m, 2H), 4.27 – 4.21 (m, 1H), 4.07 – 4.02 (m, 2H), 3.69 (s, 3H), 3.60 – 3.57 (m, 1H), 3.48 – 3.35 (m, 5H), 3.26 (s, 3H), 3.10 – 3.06 (m, 2H), 2.57 (t, J = 7.7 Hz, 2H), 2.25 – 1.97 (m, 4H), 1.70 – 1.56 (m, 4H), 1.39 – 1.29 (m, 2H), 0.96 – 0.86 (m, 12H); $^{13}\text{C NMR}$ (100 MHz, CDCl_3): δ 173.29, 171.79, 171.57, 171.18, 169.76, 142.41, 135.76, 129.29, 128.49, 128.29, 128.21, 127.08, 125.62, 86.81, 85.94, 83.16, 82.63, 58.79, 58.32, 57.40, 57.27, 52.66, 52.28, 41.02, 37.96, 36.41, 35.72, 31.21, 31.13, 30.62, 28.85, 25.63, 19.24, 19.13, 18.33, 18.11; **IR** ν_{max} (neat, cm^{-1}): 3275, 2958, 2928, 1745, 1675, 1631, 1543, 1220, 1115, 1018; **MS** (ESIMS/[M+Na] $^+$): m/z (%) 761; **HRMS** (ESI/[M+Na] $^+$): Calcd for $\text{C}_{40}\text{H}_{58}\text{N}_4\text{O}_9\text{Na}^+$: 761.4096, found 761.4102. **HPLC data:** Linear gradient 50→90% B in 10 mins, total run 30 mins, t_R = 10.542 min, 93% purity.

General Procedure for the Synthesis of C-terminal Primary

Amide: First the C-terminal ester group was hydrolyzed to the corresponding acid derivative by following the general procedure as discussed earlier. Then the resulted acid was dissolved in THF (6 mL/mmol) and cooled to -20 °C. Et_3N (1.1 eq) and ClCO_2Et (1.1 eq) were added successively and the reaction mixture was stirred for 30 min at the same temperature. Then 30% aq. NH_3 (5 eq) was added to it and further stirred for 1.5 h at 0 °C. After that it was quenched with saturated aqueous NH_4Cl solution. The mixture was extracted with EtOAc and the combined organic extracts were washed with water, brine, dried over Na_2SO_4 . Solvent was concentrated *in vacuo* and purified by flash column chromatography using 100-200 mesh silica gel (1-2% MeOH in chloroform as eluant) to give the amide.

Data for 4B: Scale of reaction 250 mg, 0.30 mmol; yield 150 mg, 61%.

R_f = 0.47 (Silica gel, 5% MeOH in CHCl_3); $^1\text{H NMR}$ (400 MHz, $\text{DMSO}-d_6$): δ 8.01 – 7.81 (m, 3H), 7.74 – 7.52 (m, 2H), 7.47 (bs, 1H), 7.29 – 7.12 (m, 6H), 4.48 – 4.37 (m, 1H), 4.32 – 4.26 (m, 1H), 4.21 – 4.07 (m, 2H), 3.94 – 3.78 (m, 2H), 3.71 – 3.54 (m, 2H), 3.35 – 3.25 (m, 8H), 3.24 – 3.11 (m, 5H), 2.98 – 2.91 (m, 1H), 2.40 (t, J = 6.9 Hz, 2H), 2.17 – 1.88 (m, 9H), 1.72 – 1.61 (m, 3H), 0.92 – 0.74 (m, 18H); $^{13}\text{C NMR}$ (100 MHz, $\text{DMSO}-d_6$): δ 208.52, 172.82, 172.76, 172.71, 172.35, 171.99, 170.92, 169.79, 137.97, 129.75, 128.59, 128.45, 126.69, 87.84, 85.53, 82.65, 57.22, 57.03, 53.59, 42.87, 42.44, 34.65, 34.59, 30.17, 20.09, 20.02, 19.87, 19.72, 19.62, 18.85, 18.69, 18.13, 15.44, 14.86, 11.89, 11.77; **IR** ν_{max} (neat, cm^{-1}): 3397, 3293, 2960, 2923, 1641, 1535, 1455, 1369, 1264, 1227, 1157, 1116, 1018; **MS** (ESIMS/[M+H] $^+$): m/z (%) 803; **HRMS** (ESI/[M+H] $^+$): Calcd for $\text{C}_{41}\text{H}_{67}\text{N}_6\text{O}_{10}^+$: 803.4913, found 803.4900. **HPLC data:** Isocratic (50%), total run 25 mins, t_R = 7.350 min, 86% purity.

Data for 4E: Scale of reaction 60 mg, 0.096 mmol; yield 32 mg, 55%.

R_f = 0.5 (Silica gel, 8% MeOH in CHCl_3); $^1\text{H NMR}$ (300 MHz, $\text{DMSO}-d_6$): δ 7.88 – 7.76 (m, 2H), 7.70 (d, J = 8.6 Hz, 1H), 7.48 (d, J = 8.8 Hz, 1H), 7.37 (bs, 1H), 7.29 – 7.13 (m, 5H), 6.99 (bs, 1H), 4.48 – 4.33 (m, 1H), 4.23 – 4.03 (m, 2H), 3.64 – 3.47 (m, 1H), 3.08 – 2.93 (m, 1H), 2.82 – 2.65 (m, 2H), 2.25 – 2.08 (m, 4H), 2.06 – 1.85 (m, 4H), 1.65 – 1.29 (m, 8H), 1.11 – 0.94 (m, 1H), 0.93 – 0.69 (m, 18H); $^{13}\text{C NMR}$ (100 MHz, $\text{DMSO}-d_6$): δ 173.75, 172.46, 172.32, 171.42, 170.95, 138.69, 129.58, 128.38, 126.58, 84.80, 71.57, 58.67, 58.24, 54.19, 52.52, 38.37, 38.02, 34.97, 30.79, 30.60, 27.97, 25.26, 25.03, 19.83, 19.59, 18.72, 18.68, 17.92, 15.45, 11.86; **IR** ν_{max} (neat, cm^{-1}): 3381, 3277, 2923, 2855, 1633, 1541, 1456, 1372, 1223, 1019; **MS** (ESIMS/[M+Na] $^+$): m/z (%) 634; **HRMS** (ESI/[M+H] $^+$): Calcd for $\text{C}_{34}\text{H}_{54}\text{N}_5\text{O}_5^+$: 612.4120, found 612.4153. **HPLC data:** Isocratic (50%), total run 20 mins, t_R = 13.910 min, 100% purity.

Data for 4G: Scale of reaction 211 mg, 0.32 mmol; yield 163 mg, 79%.

R_f = 0.5 (Silica gel, 8% MeOH in CHCl_3); $^1\text{H NMR}$ (400 MHz, $\text{DMSO}-d_6$): δ 8.19 – 8.11 (m, 1H), 7.99 (d, J = 8.7 Hz, 1H), 7.83 (d, J = 8.8 Hz, 1H), 7.65 (t, J = 8.8 Hz, 1H), 7.57 (d, J = 8.4 Hz, 1H), 7.46 (bs, 1H), 7.27 – 7.15 (m, 5H), 4.47 – 4.37 (m, 1H), 4.30 (d, J = 1.9 Hz, 1H), 4.22 – 4.13 (m, 2H), 3.93 – 3.88 (m, 1H), 3.83 (t, J = 1.8 Hz, 1H), 3.66 – 3.61 (m, 1H), 3.33 (s, 3H), 3.17 – 3.14 (m, 5H), 2.99 – 2.91 (m, 2H), 2.22 – 1.88 (m, 5H), 1.54 – 1.44 (m, 4H), 1.31 – 1.17 (m, 4H), 0.88 – 0.79 (m, 12H); $^{13}\text{C NMR}$ (100 MHz, $\text{DMSO}-d_6$): δ 172.79, 172.67, 171.54, 171.48, 169.72, 137.94, 129.77, 128.44, 126.68, 87.67, 85.22, 83.36, 82.82, 82.70, 58.31, 58.03, 57.21, 57.04, 53.57, 35.60, 31.28, 30.48, 25.58, 22.34, 19.76, 19.61, 18.67, 18.52, 14.31; **IR** ν_{max} (neat, cm^{-1}): 3396, 3293, 2959, 2928, 1643, 1535, 1456, 1224, 1108, 1018; **MS** (ESIMS/[M+Na] $^+$): m/z (%) 670; **HRMS** (ESI/[M+H] $^+$): Calcd for $\text{C}_{33}\text{H}_{54}\text{N}_5\text{O}_8^+$: 648.3967, found 648.3964. **HPLC data:** Isocratic (50%), total run 25 mins, t_R = 10.480 min, 92% purity.

Data for 4J: Scale of reaction 63 mg, 0.1 mmol; yield 52 mg, 84%.

R_f = 0.4 (Silica gel, 8% MeOH in CHCl_3); $^1\text{H NMR}$ (400 MHz, $\text{DMSO}-d_6$): δ 8.16 (t, J = 5.4 Hz, 1H), 7.91 (d, J = 8.8 Hz, 1H), 7.70 (d, J = 8.8 Hz, 1H), 7.59 (d, J = 8.3 Hz, 1H), 7.47 (bs, 1H), 7.25 – 7.15 (m, 6H), 4.47 – 4.39 (m, 1H), 4.31 (bs, 1H), 4.22 – 4.12 (m, 2H), 3.93 – 3.86 (m, 1H), 3.83 (bs, 1H), 3.64 (bs, 1H), 3.31 – 3.23 (m, 4H), 3.21 – 3.12 (m, 4H), 2.99 – 2.91 (m, 2H), 2.77 (t, J = 2.6 Hz, 1H), 2.32 – 2.10 (m,

4H), 2.01 – 1.89 (m, 2H), 1.71 – 1.61 (m, 2H), 0.87 – 0.79 (m, 12H); ¹³C NMR (100 MHz, DMSO-*d*₆): δ 172.71, 172.16, 171.52 (2C), 169.74, 137.96, 129.81, 128.48, 126.73, 87.65, 85.19, 84.59, 82.84, 82.73, 71.93, 58.34, 58.08, 57.24, 57.07, 53.59, 37.83, 34.54, 31.23, 30.53, 24.99, 19.79, 19.65, 18.69, 18.60, 17.85; IR *v*_{max} (neat, cm⁻¹): 3295, 2923, 2853, 1644, 1529, 1447, 1219, 1112, 1018; MS (ESIMS/[M+Na]⁺): *m/z*(%) 666; HRMS (ESI/[M+Na]⁺): Calcd for C₃₃H₄₉N₅O₈Na⁺ : 666.3473, found 666.3480. HPLC data: Linear gradient 50→90% B in 10 mins, total run 25 mins, *t*_R = 9.890 min, 92% purity.

Data for 4M: Scale of reaction 170 mg, 0.25 mmol; yield 130 mg, 77%.

*R*_f = 0.5 (Silica gel, 8% MeOH in CHCl₃); ¹H NMR (400 MHz, DMSO-*d*₆): δ 8.15 (t, *J* = 5.3 Hz, 1H), 7.84 (d, *J* = 8.8 Hz, 1H), 7.69 (d, *J* = 8.7 Hz, 1H), 7.58 (d, *J* = 8.3 Hz, 1H), 7.47 (bs, 1H), 7.25 – 7.13 (m, 6H), 4.47 – 4.39 (m, 1H), 4.30 (bs, 1H), 4.22 – 4.13 (m, 2H), 3.93 – 3.86 (m, 1H), 3.82 (bs, 1H), 3.63 (bs, 1H), 3.31 – 3.23 (m, 4H), 3.22 – 3.11 (m, 4H), 2.99 – 2.91 (m, 2H), 2.21 – 2.07 (m, 2H), 2.00 – 1.88 (m, 2H), 1.52 – 1.42 (m, 2H), 1.29 – 1.16 (m, 8H), 0.87 – 0.79 (m, 15H); ¹³C NMR (100 MHz, DMSO-*d*₆): δ 172.79, 172.69, 171.57, 171.50, 169.73, 137.96, 129.80, 128.47, 126.71, 87.65, 85.19, 82.83, 82.71, 58.23, 58.03, 57.23, 57.07, 53.58, 37.83, 35.64, 31.69, 31.24, 30.53, 29.03, 28.94, 25.93, 22.54, 19.79, 19.64, 18.69, 18.56, 14.44; IR *v*_{max} (neat, cm⁻¹): 3283, 2957, 2926, 1670, 1634, 1542, 1106, 1018; MS (ESIMS/[M+H]⁺): *m/z*(%) 676; HRMS (ESI/[M+H]⁺): Calcd for C₃₅H₅₈N₅O₈⁺ : 676.4280, found 676.4286. HPLC data: Linear gradient 50→90% B in 10 mins, total run 20 mins, *t*_R = 10.272 min, 97% purity.

Data for 4P: Scale of reaction 210 mg, 0.29 mmol; yield 161 mg, 78%.

*R*_f = 0.45 (Silica gel, 8% MeOH in CHCl₃); ¹H NMR (400 MHz, DMSO-*d*₆): δ 8.15 (t, *J* = 5.8 Hz, 1H), 7.84 (d, *J* = 8.8 Hz, 1H), 7.68 (d, *J* = 8.7 Hz, 1H), 7.58 (d, *J* = 8.4 Hz, 1H), 7.47 (bs, 1H), 7.24 – 7.15 (m, 6H), 4.46 – 4.39 (m, 1H), 4.32 – 4.28 (m, 1H), 4.21 – 4.13 (m, 2H), 3.92 – 3.86 (m, 1H), 3.85 – 3.79 (m, 1H), 3.66 – 3.60 (m, 1H), 3.31 – 3.23 (m, 4H), 3.22 – 3.11 (m, 4H), 2.99 – 2.89 (m, 2H), 2.21 – 2.06 (m, 2H), 2.01 – 1.89 (m, 2H), 1.52 – 1.42 (m, 2H), 1.25 – 1.20 (m, 12H), 0.88 – 0.79 (m, 15H); ¹³C NMR (75 MHz, DMSO-*d*₆): δ 172.77, 172.65, 171.51, 171.45, 169.69, 137.92, 129.75, 128.43, 126.67, 87.66, 85.21, 82.79, 82.67, 79.62, 58.24, 58.00, 57.19, 57.02, 53.54, 37.83, 35.62, 31.72, 31.19, 30.45, 29.36, 29.24, 29.09, 29.02, 25.88, 22.53, 19.75, 19.59, 18.64, 18.49, 14.38; IR *v*_{max} (neat, cm⁻¹): 3285, 2958, 2925, 2854, 1638, 1541, 1455, 1219, 1115, 1019; MS (ESIMS/[M+Na]⁺): *m/z*(%) 726; HRMS (ESI/[M+Na]⁺): Calcd for C₃₇H₆₁N₅O₈Na⁺ : 726.4412, found 726.44415. HPLC data: Linear gradient 50→90% B in 10 mins, total run 20 mins, *t*_R = 10.316 min, 98% purity.

Data for 4S: Scale of reaction 140 mg, 0.19 mmol; yield 111 mg, 81%.

*R*_f = 0.49 (Silica gel, 5% MeOH in CHCl₃); ¹H NMR (300 MHz, DMSO-*d*₆): δ 8.24 – 8.10 (m, 1H), 7.85 (d, *J* = 8.8 Hz, 1H), 7.72 – 7.64 (m, 1H), 7.58 (d, *J* = 8.4 Hz, 1H), 7.47 (bs, 1H), 7.31 – 7.12 (m, 6H), 5.85 – 5.70 (m, 1H), 5.03 – 4.89 (m, 2H), 4.78 – 4.35 (m, 1H), 4.32 – 4.25 (m, 1H), 4.24 – 4.09 (m, 3H), 3.93 – 3.86 (m, 1H), 3.85 – 3.78 (m,

1H), 3.68 – 3.58 (m, 1H), 3.40 – 3.04 (m, 7H), 3.01 – 2.87 (m, 2H), 2.23 – 1.89 (m, 4H), 1.54 – 1.40 (m, 2H), 1.37 – 1.18 (m, 10H), 0.87 – 0.79 (m, 12H); ¹³C NMR (100 MHz, DMSO-*d*₆): δ 172.76, 172.66, 171.52, 169.70, 139.27, 137.93, 129.76, 128.44, 126.68, 115.09, 87.65, 85.20, 82.80, 82.67, 58.23, 58.02, 57.21, 57.04, 53.55, 37.83, 35.61, 33.62, 31.21, 30.48, 29.05, 28.99, 28.88, 28.67, 25.87, 19.76, 19.61, 18.66, 18.52; IR *v*_{max} (neat, cm⁻¹): 3396, 3291, 2926, 2856, 1639, 1535, 1450, 1221, 1114, 1018; MS (ESIMS/[M-1]⁺): *m/z*(%) 700; HRMS (ESI/[M+Na]⁺): Calcd for C₃₇H₅₉N₅O₈Na⁺ : 724.4256, found 724.4279. HPLC data: Linear gradient 50→90% B in 10 mins, total run 20 mins, *t*_R = 10.590 min, 94% purity.

Data for 4V: Scale of reaction 200 mg, 0.27 mmol; yield 155 mg, 79%.

*R*_f = 0.6 (Silica gel, 5% MeOH in CHCl₃); ¹H NMR (400 MHz, CDCl₃): δ 8.16 (t, *J* = 5.6 Hz, 1H), 7.85 (d, *J* = 8.8 Hz, 1H), 7.69 (d, *J* = 8.7 Hz, 1H), 7.59 (d, *J* = 8.4 Hz, 1H), 7.47 (bs, 1H), 7.29 – 7.12 (m, 11H), 4.47 – 4.40 (m, 1H), 4.32 – 4.29 (m, 1H), 4.22 – 4.15 (m, 2H), 3.92 – 3.87 (m, 1H), 3.84 – 3.81 (m, 1H), 3.65 – 3.62 (m, 1H), 3.31 – 3.24 (m, 4H), 3.21 – 3.13 (m, 4H), 3.00 – 2.89 (m, 2H), 2.54 (t, *J* = 7.6 Hz, 2H), 2.22 – 2.07 (m, 2H), 2.00 – 1.89 (m, 2H), 1.59 – 1.47 (m, 4H), 1.30 – 1.21 (m, 2H), 0.87 – 0.79 (m, 12H); ¹³C NMR (100 MHz, DMSO-*d*₆): δ 172.75, 172.69, 171.54, 171.49, 169.73, 142.73, 137.95, 129.79, 128.72, 128.67, 128.46, 126.70, 126.06, 87.67, 85.21, 82.83, 82.71, 58.24, 58.04, 57.22, 57.06, 53.58, 37.84, 35.58, 35.55, 31.25, 30.52, 28.70, 25.75, 19.79, 19.64, 18.68, 18.56; IR *v*_{max} (neat, cm⁻¹): 3395, 3292, 2926, 2855, 1640, 1535, 1455, 1112, 1018; MS (ESIMS/[Na]⁺): *m/z*(%) 746; HRMS (ESI/[M+Na]⁺): Calcd for C₃₉H₅₇N₅O₈Na⁺ : 746.4099, found 746.4100. HPLC data: Linear gradient 50→90% B in 10 mins, total run 20 mins, *t*_R = 10.272 min, 96% purity.

General Procedure for Permethylolation: To a stirring solution of compound in dry DMF (3 mL/mmol) at 0 °C Ag₂O (2 eq) and MeI (2.5 eq) were sequentially added. After stirring for 12 h at room temperature, the reaction mixture was diluted with EtOAc, filtered to remove the silver oxide, washed with saturated aqueous Na₂S₂O₃ solution, water, brine, dried (Na₂SO₄), filtered and concentrated in *vacuo*. Purification by silica gel (100-200 mesh) column chromatography (0.5-1.5% MeOH in chloroform as eluant) afforded the permethylated compound.

Data for 4C: Scale of reaction 80 mg, 0.1 mmol; yield 66 mg, 73%.

*R*_f = 0.51 (Silica gel, 4% MeOH in CHCl₃); ¹H NMR (400 MHz, DMSO-*d*₆): δ 7.34-7.13 (m, 5H), 5.56-5.37 (m, 1H), 5.14-4.9 (m, 2H), 4.67-4.47 (m, 1H), 4.41-4.29 (m, 1H), 4.28-4.12 (m, 1H), 3.77-3.48 (m, 2H), 3.39-3.26 (m, 6H), 3.25-3.07 (m, 5H), 3.05-2.56 (m, 24H), 2.34-2.14 (m, 6H), 2.13-2.04 (m, 4H), 1.96-1.62 (m, 4H), 0.94-0.63 (m, 18H); ¹³C NMR (100 MHz, DMSO-*d*₆): δ 211.99, 174.87, 172.79, 172.68, 170.27, 170.13, 168.92, 137.89, 129.61, 128.49, 126.73, 85.07, 84.34, 70.24, 58.22, 58.01, 54.95, 47.04, 45.85, 36.58, 35.76, 31.94, 31.72, 30.21, 30.03, 29.44, 28.46, 26.97, 26.81, 22.51, 19.66, 19.48, 18.52, 18.48, 18.39, 17.85, 16.40, 16.34, 14.34, 10.67, 8.09; IR *v*_{max} (neat, cm⁻¹): 3406, 2923, 1637, 1454, 1365, 1265, 1219, 1018; MS (ESIMS/[M+Na]⁺): *m/z*(%) 923; HRMS (ESI/[M+Na]⁺): Calcd for C₄₈H₈₀N₆O₁₀Na⁺ : 923.5828, found 923.5834. HPLC data:

Linear gradient 50→90% B in 10 mins, total run 20 mins, t_R = 7.753 min, 100% purity.

Data for 4H: Scale of reaction 90 mg, 0.14 mmol; yield 75 mg, 74%.

R_f = 0.5 (Silica gel, 4% MeOH in CHCl_3); $^1\text{H NMR}$ (400 MHz, $\text{DMSO}-d_6$): δ 7.29-7.14 (m, 5H), 5.59-5.40 (m, 1H), 5.08-4.94 (m, 2H), 4.73-4.53 (m, 1H), 4.08-3.99 (m, 1H), 3.56-3.42 (m, 2H), 3.35-3.31 (m, 5H), 3.30-3.26 (m, 3H), 3.25-3.20 (m, 3H), 3.01-2.94 (m, 3H), 2.93-2.88 (m, 2H), 2.87-2.76 (m, 12H), 2.35-2.14 (m, 5H), 1.56-1.44 (m, 2H), 1.31-1.20 (m, 6H), 0.9-0.61 (m, 12H); $^{13}\text{C NMR}$ (100 MHz, $\text{DMSO}-d_6$): δ 173.14, 173.12, 170.13, 169.11, 168.63, 138.17, 129.60, 128.48, 126.61, 87.42, 87.03, 81.65, 81.44, 80.36, 58.07, 57.84, 57.24, 57.21, 54.69, 36.33, 35.70, 32.99, 31.32, 30.59, 30.30, 30.02, 26.91, 24.73, 22.34, 20.03, 19.72, 19.64, 18.40, 17.92, 14.26; **IR** ν_{max} (neat, cm^{-1}): 3410, 2959, 2927, 1640, 1463, 1404, 1098, 1018; **MS** (ESI/[M+Na] $^+$): m/z (%) 754; **HRMS** (ESI/[M+Na] $^+$): Calcd for $\text{C}_{39}\text{H}_{65}\text{N}_5\text{O}_8\text{Na}^+$: 754.4725, found 754.4739. **HPLC data:** Isocratic (50%), total run 20 mins, t_R = 13.798 min, 100% purity.

Data for 4K: Scale of reaction 20 mg, 0.03 mmol; yield 16 mg, 73%.

R_f = 0.6 (Silica gel, 6% MeOH in CHCl_3); $^1\text{H NMR}$ (400 MHz, $\text{DMSO}-d_6$): δ 7.32-7.09 (m, 5H), 5.09-4.89 (m, 1H), 4.78-4.49 (m, 2H), 4.48-4.27 (m, 1H), 4.21-3.99 (m, 1H), 3.74-3.51 (m, 2H), 3.44-3.19 (m, 14H), 3.07-2.64 (m, 14H), 2.56-2.52 (m, 1H), 2.38-2.08 (m, 4H), 2.07-1.84 (m, 2H), 1.32-1.16 (m, 2H), 0.92-0.55 (m, 12H); **IR** ν_{max} (neat, cm^{-1}): 3396, 2958, 2924, 2853, 1722, 1642, 1456, 1413, 1261, 1219, 1100, 1018; **MS** (ESI/[M] $^+$): m/z (%) 727; **HRMS** (ESI/[M] $^+$): Calcd for $\text{C}_{39}\text{H}_{61}\text{N}_5\text{O}_8^+$: 727.4515, found 727.4524. **HPLC data:** Linear gradient 50→90% B in 10 mins, total run 20 mins, t_R = 13.640 min, 91% purity.

Data for 4N: Scale of reaction 60 mg, 0.09 mmol; yield 52 mg, 76%.

R_f = 0.55 (Silica gel, 3% MeOH in CHCl_3); $^1\text{H NMR}$ (400 MHz, $\text{DMSO}-d_6$): δ 7.29-7.12 (m, 5H), 5.53-5.38 (m, 1H), 5.09-4.93 (m, 2H), 4.75-4.54 (m, 1H), 4.08-3.99 (m, 1H), 3.59-3.45 (m, 2H), 3.37-3.19 (m, 9H), 3.19-3.03 (m, 2H), 3.02-2.88 (m, 6H), 2.87-2.74 (m, 11H), 2.37-2.13 (m, 4H), 1.56-1.44 (m, 2H), 1.30-1.19 (m, 8H), 0.89-0.62 (m, 15H); $^{13}\text{C NMR}$ (100 MHz, $\text{DMSO}-d_6$): δ 173.16, 170.12, 169.54, 168.65, 138.24, 129.69, 128.55, 126.67, 87.43, 81.74, 80.42, 79.67, 58.12, 57.87, 57.28, 54.76, 36.49, 36.39, 35.76, 33.06, 31.71, 30.65, 30.35, 30.06, 29.11, 28.99, 26.96, 25.11, 22.53, 20.12, 19.79, 18.46, 17.99, 14.43; **IR** ν_{max} (neat, cm^{-1}): 3427, 2927, 2856, 1642, 1463, 1403, 1218, 1099, 1018; **MS** (ESI/[Na] $^+$): m/z (%) 782; **HRMS** (ESI/[M+H] $^+$): Calcd for $\text{C}_{41}\text{H}_{69}\text{N}_5\text{O}_8\text{Na}^+$: 782.5038, found 782.5043. **HPLC data:** Isocratic (50%), total run 20 mins, t_R = 13.872 min, 94% purity.

Data for 4Q: Scale of reaction 70 mg, 0.1 mmol; yield 58 mg, 74%.

R_f = 0.66 (Silica gel, 5% MeOH in CHCl_3); $^1\text{H NMR}$ (400 MHz, $\text{DMSO}-d_6$): δ 7.32-7.12 (m, 5H), 5.52-5.41 (m, 1H), 5.10-4.94 (m, 2H), 4.73-4.58 (m, 1H), 4.17-4.00 (m, 1H), 3.57-3.38 (m, 2H), 3.36-3.21 (m, 15H), 3.01-2.89 (m, 4H), 2.86-2.78 (m, 9H), 2.35-2.14 (m, 4H), 1.55-1.44 (m, 2H), 1.29-1.18 (m, 12H), 0.89-0.62 (m, 15H); $^{13}\text{C NMR}$ (100 MHz, $\text{DMSO}-d_6$): δ 173.09, 170.10, 169.11, 168.63, 167.93, 138.17, 129.60, 128.47, 126.59, 87.43, 87.04, 82.38, 81.65, 58.08, 57.84, 57.24, 57.21, 54.69, 36.46, 36.44, 36.33, 35.69, 35.03, 33.01, 31.70, 30.59, 30.29, 30.01, 29.35, 29.26, 29.08, 29.06, 25.04, 22.51, 20.03, 19.72, 18.38, 17.92, 14.32; **IR** ν_{max} (neat, cm^{-1}): 3407, 2926, 2856,

1718, 1641, 1462, 1403, 1103, 1018; **MS** (ESI/[Na] $^+$): m/z (%) 811; **HRMS** (ESI/[M+Na] $^+$): Calcd for $\text{C}_{43}\text{H}_{73}\text{N}_5\text{O}_8\text{Na}^+$: 810.5351, found 810.5356. **HPLC data:** Isocratic (50%), total run 20 mins, t_R = 13.923 min, 100% purity.

Data for 4T: Scale of reaction 60 mg, 0.08 mmol; yield 52 mg, 77 %.

R_f = 0.7 (Silica gel, 5% MeOH in CHCl_3); $^1\text{H NMR}$ (400 MHz, $\text{DMSO}-d_6$): δ 7.34-7.10 (m, 5H), 5.84-5.72 (m, 1H), 5.52-5.38 (m, 1H), 5.08-4.89 (m, 4H), 4.75-4.59 (m, 1H), 4.22-3.88 (m, 2H), 3.58-3.44 (m, 2H), 3.36-3.21 (m, 9H), 3.03-2.75 (m, 15H), 2.36-2.13 (m, 5H), 2.04-1.96 (m, 2H), 1.55-1.43 (m, 2H), 1.38-1.19 (m, 10H), 0.89-0.61 (m, 12H); $^{13}\text{C NMR}$ (100 MHz, $\text{DMSO}-d_6$): δ 173.17, 170.13, 169.60, 169.14, 168.66, 139.29, 138.24, 129.69, 128.56, 126.69, 115.13, 87.43, 87.04, 79.67, 58.14, 57.88, 57.29, 54.77, 36.49, 36.39, 35.77, 35.04, 33.65, 33.03, 30.66, 30.36, 30.07, 29.14, 29.10, 28.92, 28.69, 27.01, 2508, 20.12, 19.81, 18.47, 18.00; **IR** ν_{max} (neat, cm^{-1}): 3403, 2928, 2855, 1717, 1640, 1462, 1405, 1103, 1018; **MS** (ESI/[Na] $^+$): m/z (%) 808; **HRMS** (ESI/[M+Na] $^+$): Calcd for $\text{C}_{43}\text{H}_{71}\text{N}_5\text{O}_8\text{Na}^+$: 808.5195, found 808.5199. **HPLC data:** Isocratic (50%), total run 20 mins, t_R = 10.831 min, 100% purity.

Data for 4W: Scale of reaction 80 mg, 0.11 mmol; yield 67 mg, 74%.

R_f = 0.8 (Silica gel, 4% MeOH in CHCl_3); $^1\text{H NMR}$ (400 MHz, $\text{DMSO}-d_6$): δ 7.29-7.13 (m, 10H), 5.53-5.38 (m, 1H), 5.07-4.94 (m, 2H), 4.74-4.58 (m, 1H), 4.07-3.99 (m, 1H), 3.58-3.45 (m, 2H), 3.36-3.22 (m, 17H), 3.00-2.89 (m, 2H), 2.83-2.78 (m, 9H), 2.57-2.52 (m, 2H), 2.35-2.27 (m, 2H), 2.25-2.14 (m, 2H), 1.60-1.48 (m, 4H), 1.33-1.25 (m, 2H), 0.87-0.61 (m, 12H); $^{13}\text{C NMR}$ (100 MHz, $\text{DMSO}-d_6$): δ 173.06, 170.09, 169.59, 169.12, 168.63, 142.62, 138.18, 129.61, 128.66, 128.61, 128.49, 126.62, 126.02, 87.42, 87.03, 81.65, 80.36, 58.09, 57.85, 57.25, 57.22, 54.70, 36.45, 36.33, 35.72, 35.56, 35.02, 32.94, 31.20, 30.61, 30.28, 30.02, 28.76, 26.96, 26.90, 24.87, 22.51, 20.04, 19.74, 18.40, 17.92; **IR** ν_{max} (neat, cm^{-1}): 3479, 2959, 2930, 1716, 1640, 1460, 1405, 1257, 1102, 1019; **MS** (ESI/[Na] $^+$): m/z (%) 830; **HRMS** (ESI/[M+Na] $^+$): Calcd for $\text{C}_{45}\text{H}_{69}\text{N}_5\text{O}_8\text{Na}^+$: 830.5038, found 830.5036. **HPLC data:** Isocratic (50%), total run 30 mins, t_R = 13.663 min, 92% purity.

Assays for *In vitro* Activity against Intra-macrophagic

Amastigotes: Murine macrophages (J-774A.1 cell line) were seeded in 96-well plates at a density of $4 \times 10^4/\text{mL}/100\mu\text{L}/\text{well}$ and incubated at 37°C in a CO_2 incubator. After 24 h, cells were infected with WHO reference strain (MHOM/IN/80/Dd8) of promastigotes (expressing luciferase firefly reporter gene) at 1:10 ratio (1 macrophage: 10 promastigotes). After incubation for 24 h, the plates were washed with fresh media to remove un-internalized extracellular promastigotes. The infected macrophages were incubated with the synthetic peptides at two-fold dilutions up to seven concentrations starting from 100 μM and the plates were incubated for 72 h. Miltefosine was used as a reference drug. After incubation, the compounds containing medium was aspirated and 50 μL of phosphate buffer saline (PBS) was added in each well and mixed with an equal amount of Steady Glo $^{\text{®}}$ reagent. The reading was taken in a luminometer after gentle shaking of plates for 2 min. After gentle shaking for 2 min, the reading was taken in a luminometer.²⁵ The values are expressed as relative luminescence

ARTICLE

Journal Name

unit (RLU) and data were transformed into a graphic program (MS Excel). 50% inhibitory concentration (IC₅₀) value of each tested compound was calculated by nonlinear regression analysis of the concentration response curve using the four parameter Hill equations.

Assays for Cytotoxicity in Mammalian Cells: Mammalian kidney fibroblast cells (Vero cell line) were used to assess the cytotoxic effect of synthetic peptides. The quantification of viable cells was measured by 3-(4,5-dimethyl-2-thiazolyl)-2,5-diphenyl-2H-tetrazolium bromide (MTT) assay.²⁶ Vero cells (1 × 10⁵/mL/100 µL/well) were seeded in 96-well plates and incubated at 37 °C in a CO₂ incubator. After 24 h, test compounds were added at three-fold dilutions in complete medium up to seven concentrations starting from 400 µM and plates were incubated at 37 °C in a CO₂ incubator. Podophyllotoxin was used as a reference drug. After 72 h, 25 µL of MTT reagent (Sigma-Aldrich, USA) (5 mg/mL) was added to each well and incubated at 37 °C for 2 h. At the end of the incubation, the supernatant were removed and 150 µL of pure DMSO was added to each well for solubilising the formazan crystal. After 15 min of gentle shaking, the readings were recorded as absorbance at 544 nm on a micro plate reader. The cell viability was determined based on the optical absorbance of the treated and untreated samples and of blank wells using a graphic program (MS Excel). The fifty percent cytotoxic concentration (CC₅₀) values were estimated as described by Huber and Koella.²⁷ The selectivity index was determined by calculating the ratio between Cytotoxicity (CC₅₀) and antileishmanial activity (IC₅₀).

Structure-Activity Relationship studies: Molecules were drawn and minimized in MOE followed by partial charge calculation using AMBER99. Structures were subsequently subjected to molecular dynamics simulation at 300 K and AMBER99 force field in vacuum with 100 ps of equilibrium run followed by production run for 500 ps. Resulting structures were analysed in Chimera.

Acknowledgements

We gratefully acknowledge the financial support by DST, New Delhi, India for JC Bose Fellowship (TKC, DST No.: SR/S2/JCB-30/2007). The authors wish to thank CSIR, New Delhi (D.D.) and IISc, Bangalore (H.P.A.K.) for research fellowships. The authors are thankful to SAIF, CSIR-CDRI and Department of Organic Chemistry, IISc for providing the spectroscopic and analytical data, also Mr. R. K. Purshottam, CSIR-CDRI for HPLC data.

Notes and references

- (a) D. Butler, *Nature*, 2007, **449**, 158–159; (b) A. Cavalli and M. L. Bolognesi, *J. Med. Chem.*, 2009, **52**, 7339–7359.
- F. Chappuis, S. Sundar and A. Hailu, H. Ghalib, J. Alvar, M. Boelaer, *Nature Rev. Microbiol.*, 2007, **5**, 873–885.
- R. D. Pearson, A. de Queiroz Sousa, *Clin. Infect. Dis.*, 1996, **22**, 1–11. DOI: 10.1039/C6OB02610A
- T. K. Jha, *Indian J. Med. Res.*, 2006, **123**, 389–398.
- (a) S. Sundar and M. Rai, *Curr. Opin. Infect. Dis.*, 2002, **15**, 593–598; (b) R. Pink, A. Hudson, M. A. Mouries, M. Bending, *Nat. Rev. Drug Discovery*, 2005, **4**, 727–740.
- (a) S. L. Croft, S. Sundar and A. H. Fairlam, *Clin. Microbiol. Rev.*, 2006, **111**–126; (b) S. Sundar, *Trop. Med. Int. Health*, 2001, **6**, 849–854.
- (a) L. G. Rocha, J. R. G. S. Almeida, R. O. Mace and J. M. Barbosa-Filho, *Phytomed.*, 2005, **12**, 514–535; (b) J. N. Sangshetti, F. A. K. Khan, A. A. Kulkarni, R. Arote and R. H. Patil, *RSC Adv.*, 2015, **5**, 32376–32415; (c) R. Rajasekaran and Y.-P. P. Chen, *Drug Discov. Today*, 2015, **20**, 958–968; (d) K. Katsuno, J. N. Burrows, K. Duncan, R. H. van Huijsduijnen, T. Kaneko, K. Kita, C. E. Mowbray, D. Schmatz, P. Warner and B. T. Slingsby, *Nat. Rev. Drug Discov.*, 2015, **14**, 751–758.
- (a) E. V. Costa, M. L. B. Pinheiro, C. M. Xavier, J. R. A. Silva, A. F. Amaral, A. D. L. Souza, A. Barison, F. R. Campos, A. G. Ferreira, G. M. C. Machado, L. P. L. Leon, *J. Nat. Prod.*, 2006, **69**, 292–294; (b) R. Akue-Gedu, E. Debiton, Y. Ferandin, L. Meijer, M. Prudhomme, F. Anizon, P. Moreau, *Bioorg. Med. Chem.*, 2009, **17**, 4420–4424; (c) L. M. Sanchez, D. Lopez, B. A. Vesely, G. D. Togna, W. H. Gerwick, D. E. Kyle, R. G. Linington, *J. Med. Chem.*, 2010, **53**, 4187–4197; (d) M. Balasegaram, H. Young, F. Chappuis, G. Priotto, M. E. Raguenaud, F. Checchi, *Trans. R. Soc. Trop. Med. Hyg.*, 2009, **103**, 280–290; (e) U. Muh, M. Schuster, R. Heim, A. Singh, E. R. Olson, E. P. Greenberg, *Antimicrob. Agents Chemother.*, 2006, **50**, 3674–3679; (f) C. Vitale, G. Mercurio, C. Castiglioni, A. Cornoldi, A. Tulli, M. Fini, M. Volterrani, G. M. C. Rosano, *Cardiovasc. Diabetol.*, 2005, **4**, 6–13; (g) P. Sivaprakasam, P. N. Tosso, R. J. Doerksen, *J. Chem. Inf. Model*, 2009, **49**, 1787–1796; (h) G. Rastelli, W. Sirawaraporn, P. Sompornpisut, T. Vilaivan, S. Kamchonwongpaisan, R. Quarrell, G. Lowe, Y. Thebtaranonth, Y. Yuthavong, *Bioorg. Med. Chem.*, 2000, **8**, 1117–1128; (i) P. Khare, A. K. Gupta, P. K. Gajula, K. Y. Sunkari, A. K. Jaiswal, S. Das, P. Bajpai, T. K. Chakraborty, A. Dube and A. K. Saxena, *J. Chem. Inf. Model.*, 2012, **52**, 777–791.
- L. M. Sanchez, G. M. Knudsen, C. Helbig, G. D. Muylder, S. M. Mascuch, Z. B. Mackey, L. Gerwick, C. Clayton, J. H. Mckerrow, R. G. Linington, *J. Nat. Prod.*, 2013, **76**, 630–641.
- For reviews on sugar amino acids and tetrahydrofuran amino acids see: (a) V. Rjabovs, M. Turks, *Tetrahedron*, 2013, **69**, 10693–10710; (b) M. Risseuw, M. Overhand, G. W. J. Fleet, M. I. Simone, *Amino Acids*, 2013, **45**, 613–689; (c) M. D. P. Risseuw, M. Overhand, G. W. J. Fleet, M. I. Simone, *Tetrahedron: Asymmetry*, 2007, **18**, 2001–2010; (d) K. J. Jensen, J. Brask, *Pept. Sci.*, 2005, **80**, 747–761; (e) T. K. Chakraborty, P. Srinivasu, S. Tapadar, B. K. Mohan, *Glycoconjugate J.*, 2005, **22**, 83–93; (f) T. K. Chakraborty, P. Srinivasu, S. Tapadar, B. K. Mohan, *J. Chem. Sci.*, 2004, **116**, 187–207; (g) S. A. W. Gruner, E. Locardi, E. Lohof, H. Kessler, *Chem. Rev.*, 2002, **102**, 491–514; (h) F. Schweizer, *Angew. Chem., Int. Ed.*, 2002, **41**, 230–253; (i) T. K. Chakraborty, S. Ghosh, S. Jayaprakash, *Curr. Med. Chem.*, 2002, **9**, 421–435; (j) T. K. Chakraborty, S. Jayaprakash, S. Ghosh, *Comb. Chem. High Throughput Screening*, 2002, **5**, 373–387; (k) F. Peri, L. Cipolla, E. Forni, B. La Ferla, F. Nicotra, *Chemtracts: Org. Chem.*, 2001, **14**, 481–499 (l) J. Gervay-Hague, T. M. Weathers, *Pyranosyl Sugar Amino Acid Conjugates: Their*

- Biological Origins, Synthetic Preparations And Structural Characterisation In Glycochemistry: Principles, Synthesis and Applications*, ed. P. G. Wang, Dekker Bertozzi, C. R. New York, 2001.
- 11 (a) T. K. Chakraborty, S. Jayaprakash, P. V. Diwan, R. Nagaraj, S. R. B. Jampani, A. C. Kunwar, *J. Am. Chem. Soc.*, 1998, **120**, 12962–12963; (b) T. K. Chakraborty, S. Ghosh, S. Jayaprakash, J. A. R. P. Sharma, V. Ravikanth, P. V. Diwan, R. Nagaraj, A. C. Kunwar, *J. Org. Chem.*, 2000, **65**, 6441–6457; (c) T. K. Chakraborty, S. Jayaprakash, P. Srinivasu, M. G. Chary, P. V. Diwan, R. Nagaraj, A. R. Shankar, A. C. Kunwar, *Tetrahedron Lett.*, 2000, **41**, 8167–8171; (d) T. K. Chakraborty, S. U. Kumar, B. K. Mohan, G. D. Sarma, U. M. Kiran, B. Jagadeesh, *Tetrahedron Lett.*, 2007, **48**, 6945–6950.
 - 12 P. K. Gajula, J. Asthana, D. Panda and T. K. Chakraborty, *J. Med. Chem.*, 2013, **56**, 2235–2245.
 - 13 H. K. Majumder, *Drug targets in kinetoplastid parasites in Adv. Exp. Med. Biol.*, 2008, **625**, 1–45.
 - 14 (a) L. Luis, M. L. Serrano, M. Hidalgo and A. Mendoza-León, *BioMed. Res. Int.*, 2013, Article ID 843748; (b) A. Massarotti, A. Coluccia, R. Silvestri, G. Sorba, A. Brancale, *ChemMedChem*, 2012, **7**, 33–42; (c) B. J. Fennell, J. A. Naughton, J. Barlow, G. Brennan, I. Fairweather, E. Hoey, N. McFerran, A. Trudgett, A. Bell, *Expert Opin. Drug Discov.*, 2008, **3**, 501–518.
 - 15 K. Omura, D. Swern, *Tetrahedron*, 1978, **34**, 1651–1660.
 - 16 (a) S. Bera, G. Panda, *Org. Biomol. Chem.*, 2014, **12**, 3976–3985; (b) M. Drag, R. Latajka, E. Gumiennaa-Kontecka, H. Kozlowski, P. Kafarski, *Tetrahedron: Asymmetry*, 2003, **14**, 1837–1845; (c) S. M. Mali, M. G. Kumar, M. M. Katariya, H. N. Gopi, *Org. Biomol. Chem.*, 2014, **12**, 8462–8472.
 - 17 Ø. Jacobsen, J. Klaveness, O. P. Ottersen, M. R. Amiry-Moghaddam, P. Rongved, *Org. Biomol. Chem.*, 2009, **7**, 1599–1611.
 - 18 For some recent works see: (a) E. Marcucci, J. Tulla-Puche, F. Albericio, *Org. Lett.*, 2012, **14**, 612–615; (b) J. G. Beck, J. Chatterjee, B. Laufer, M. U. Kiran, A. O. Frank, S. Neubauer, O. Ovadia, S. Greenberg, C. Gilon, A. Hoffman, H. Kessler, *J. Am. Chem. Soc.*, 2012, **134**, 12125–12133; (c) J. Chatterjee, F. Rechenmacher, H. Kessler, *Angew. Chem., Int. Ed.*, 2013, **52**, 254–269; (d) Y. Li, N. Bionda, A. Yongye, P. Geer, M. Stawikowski, P. Cudic, K. Martinez, R. A. Houghten, *ChemBioChem*, 2013, **8**, 1865–1872; (e) A. Adamska, B. Kolesińska, A. Kluczyk, Z. J. Kamińkib, A. Janeckaa, *J. Pept. Sci.*, 2015, **21**, 807–810; (f) U. K. Marelli, J. Bezençon, E. Puig, B. Ernst, H. Kessler, *Chem. Eur. J.*, 2015, **21**, 8023–8027; (g) C. Paissoni, M. Ghitti, L. Belvisi, A. Spitaleri, G. Musco, *Chem. Eur. J.*, 2015, **21**, 14165–14170; (h) A. T. Bockus, J. A. Schwochert, C. R. Pye, C. E. Townsend, V. Sok, M. A. Bednarek, R. S. Lokey, *J. Med. Chem.*, 2015, **58**, 7409–7418; (i) T. A. Hilimire, R. P. Bennett, R. A. Stewart, P. Garcia-Miranda, A. Blume, J. Becker, N. Sherer, E. D. Helms, S. E. Butcher, H. C. Smith, B. L. Miller, *ACS Chem Biol.*, 2016, **11**, 88–94.
 - 19 I. O. Donkor, J. Han, X. Zheng, *J. Med. Chem.*, 2004, **47**, 72–79.
 - 20 L. Aurelio, R. T. C. Brownlee, A. B. Hughes, *Chem. Rev.*, 2004, **104**, 5823–5846.
 - 21 Molecular Operating Environment (MOE), 2013.08; Chemical Computing Group Inc., 1010 Sherbooke St. West, Suite #910, Montreal, QC, Canada, H3A 2R7, 2016.
 - 22 A second generation force field for the simulation of proteins, nucleic acids, and organic molecules; W. D. Cornell, P. Cieplak, C. I. Bayly, I. R. Gould, K. M. Merz, *J. Am. Chem. Soc.*, 1995, **117**, 5179–5197.
 - 23 UCSF Chimera—a visualization system for exploratory research and analysis; E. F. Pettersen, T. D. Goddard, C. C. Huang, G. S. Couch, D. M. Greenblatt, E. C. Meng, T. E. Ferrin, *J. Comput. Chem.*, 2004, **25**, 1605–1612.
 - 24 (a) B. R. Brooks, A. D. Mackerell, L. Nilsson, R. J. Petrella, *J. Comp. Chem.*, 2009, **30**, 1545–1615; (b) B. R. Brooks, R. E. Bruccoleri, B. D. Olafson, D. J. States, S. Swaminathan, M. Karplus, *J. Comput. Chem.*, 1983, **4**, 187–217.
 - 25 R. Shivahare, V. Korthikunta, H. Chandasana, M. K. Suthar, P. Agnihotri, P. Vishwakarma, T. K. Chaitanya, P. Kancharla, T. Khaliq, S. Gupta, R. S. Bhatta, J. V. Pratap, J. K. Saxena, S. Gupta, N. Tadigoppula, *J. Med. Chem.*, 2014, **57**, 3342–3357.
 - 26 T. Mosmann, *J. Immunol. Methods*, 1983, **65**, 55–63.
 - 27 W. Huber, J. C. Koella, *Acta Trop.*, 1993, **55**, 257–261.